Volume 2
Number 10
October 2023
Pages 1533–1772

Energy Advances

rsc.li/energy-advances

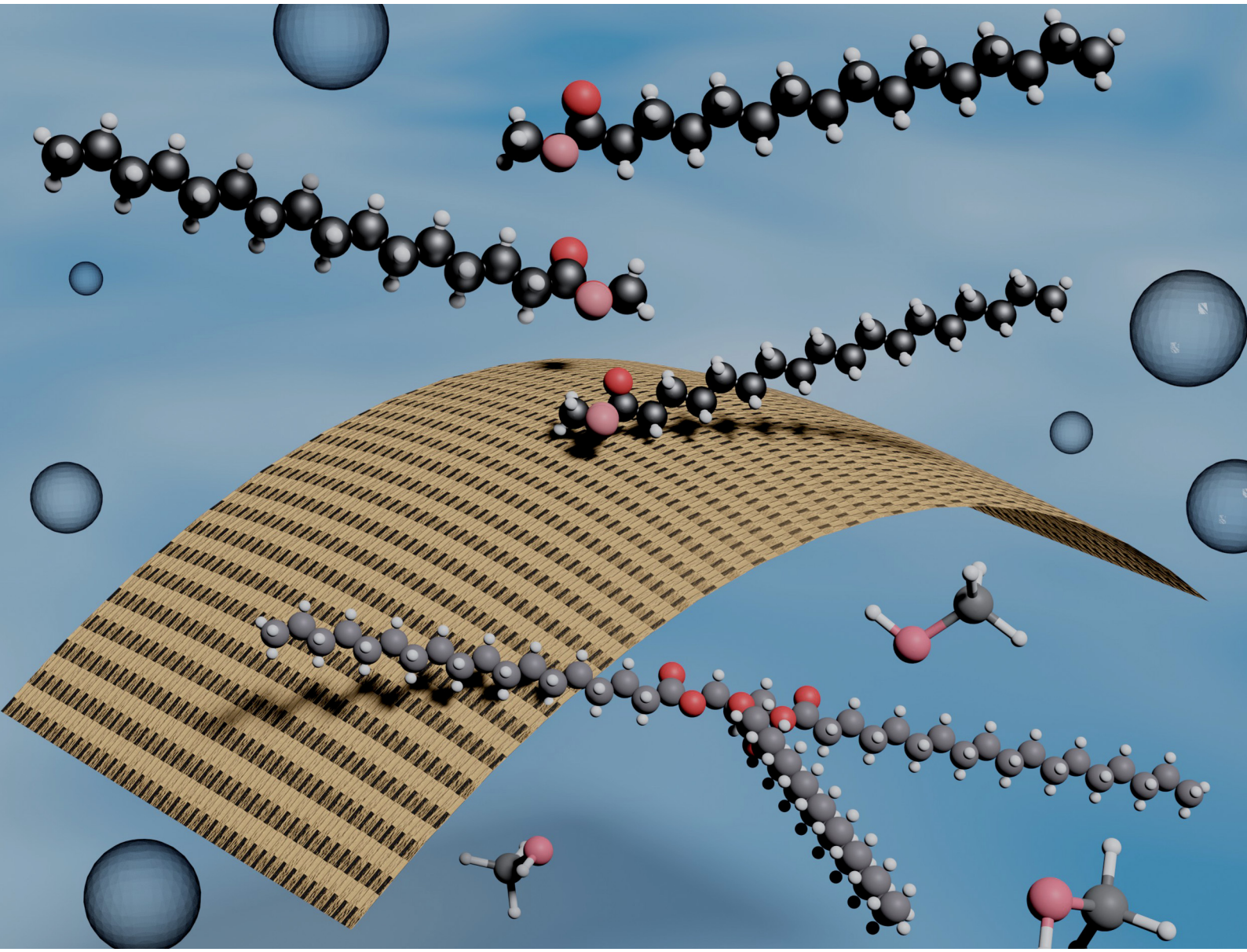

ISSN 2753-1457

ROYAL SOCIETY OF CHEMISTRY

PAPER

Katherine Huddersman *et al.*
Transesterification reaction of tristearin (TS) & glycerol mono stearate (GMS) over surface basified PAN fibrous solid catalyst

Energy Advances

ROYAL SOCIETY OF CHEMISTRY

PAPER

View Article Online
View Journal | View Issue

Cite this: *Energy Adv.*, 2023, 2, 1604

Transesterification reaction of tristearin (TS) & glycerol mono stearate (GMS) over surface basified PAN fibrous solid catalyst

Rawaz A. Ahmed, Sanaa Rashid, Ketan Ruparelia and Katherine Huddersman *

A promising solution for the near future is the substitution of non-renewable fossil fuels with sustainable liquid feedstock such as biofuel (biodiesel). The cost of conventional biodiesel production is higher than that of petroleum-based diesel production since it is produced mostly from expensive high-quality virgin oil. Conventionally, commercial biodiesel is produced *via* liquid phase base-catalyzed transesterification of the triglyceride components of the oil with short-chain alcohols. This study demonstrates the first effective conversion of the triglyceride, tristearin (TS) and the monoglyceride, glycerol monostearate (GMS) to biodiesel using novel protonated and then basified crosslinked modified polyacrylonitrile ion exchange fibres (PANF) in the form of a mesh and an investigation of their lifetime in batch recycling. 3 g of basified PANF in 26 mL of methanol with a molar ratio of methanol to tristearin (TS) of 274 : 1 at 65 °C could achieve 95% conversion of tristearin. The catalyst was re-used for 9 cycles (18 hours) before being effectively regenerated back to 70% conversion. Response surface methodology (RSM) with central composite design (CCD) gave an optimum biodiesel conversion of tristearin of 87.62% with 2.5 g of catalyst, methanol to TS molar ratio of 143 : 1 at 65 °C for 1 h (0.1936% error). Using glycerol monostearate at (a molar ratio of methanol to GMS of (115 : 1)) conversion to the methyl ester was above 97.63% at 65 °C in 60 min. These basified PANF ion exchange fibres showed comparable activity to conventional homogeneous base catalysts namely, NaOH; as well as exhibiting high stability and ease of use. The FT-IR spectra suggested that after use, active sites were blocked with most probably unreacted reactants which can be removed with a more extensive DCM washing regime. As PANF is produced in the form of a self-supporting mesh it is easy to use, regenerate *in situ*, maintain and replace in a continuous flow reactor. The study is promising as a basified catalyst for sustainable use in converting triglyceride (TGs) in fats, oils and greases (FOGs) and fatbergs in wastewater to biodiesel.

Received 3rd April 2023,
Accepted 1st August 2023

DOI: 10.1039/d3ya00145h

rsc.li/energy-advances

1. Introduction

As the availability of fossil fuel gradually declines, sustainable and renewable energy production is increasingly required with biodiesel currently being explored as an environmentally friendly substitute for diesel fuel.[1] Biodiesel can be produced *via* the following processes: (1) alkaline-catalysed transesterification (suitable for feedstocks with low free fatty acid content); (2) enzyme (biocatalyst) catalysed transesterification (3) acid-catalysed transesterification/esterification (good for feedstocks with high free fatty acid (FFA) content); (4) transesterification *via* a two-step process (again good for feedstocks with high FFA content).[2–4]

The commercial production of biodiesel from virgin oil *via* homogenous transesterification of the triglycerides uses base catalysts, most commonly, sodium hydroxide (NaOH) and potassium hydroxide (KOH). For instance, Borges *et al.*,[5] studied the homogeneous catalysis of soybean oil transesterification *via* methylic and ethylic routes in a multivariate comparison. The highest yield of biodiesel (above 90%) for the ethylic route arose from the optimum reaction parameters; reaction time 60 min, stirring 100 rpm, ethanol/oil molar ratio = 12 : 1, 0.2 wt% potassium ethoxide and temperature 35 °C. However, the biodiesel yield was 93% for the methylic route using optimum reaction parameters such as reaction time 30 min, stirring 100 rpm, methanol/oil molar ratio of 6 : 1, 0.2 wt% KOH catalyst, reaction temperature 55 °C.[5] Hariprasath *et al.*,[6] reported biodiesel production *via* the homogeneous base (NaOH) catalysis in the transesterification of cashew and canola oil. The maximum biodiesel from canola oil was 85% which was 30% higher than the biodiesel from cashew oil. The optimized transesterification parameters used to yield biodiesel from canola oil were a temperature of 70 °C for 120 min,

Faculty of Health and Life Sciences, De Montfort University, The Gateway, Leicester, LE1 9BH, UK. E-mail: huddzeo1@dmu.ac.uk

an alcohol/fatty oil molar ratio 6.5 : 1 mixing at 550 rpm.[6] Dias *et al.*[7] investigated different alkali catalysts for the transesterification of virgin and waste cooking oils. It was found that the virgin oils and waste oils produced biodiesel yields of 97 and 92% respectively.[7] The authors found that process parameters such as catalyst concentration, feedstock-to-alcohol ratio, stock purity and temperature all affect the purity and yield of the resulting biodiesel.[7] An increase in alkali concentration is also detrimental to the process as it leads to soap formation as well as excess glycerol production which dilutes the biodiesel and ultimately increases reaction time.[8] Transesterification of oil which was extracted from *Citrullus vulgaris* (watermelon) seeds has been reported as a potential feedstock in biodiesel production. Initial catalyst loading of a 0.13 g NaOH yielded 70% biodiesel; further increasing the catalyst to 0.18 g gradually reduced the yield to 49%.[9] The most recent literature has reported the transesterification of canola oil in a continuous flow reactor using homogeneous base as catalyst. The maximum yield (95.13%) was obtained using: a 9 : 1 molar ratio (methanol to oil), 0.5% (w/w) KOH, 300 rpm stirring speed, at 60 °C for 60 minutes under reflux of methanol.[10]

Unfortunately, free fatty acids in low-quality feedstocks have a negative effect on homogenous base catalysts and acid and neutralisation pre-treatment processes are required prior to use. These pre-treatments are undesirable as they add to operation costs and are not environmentally friendly. Solid catalysts are thus a favourable green and economical alternative for the conversion of waste cooking oils to biodiesel.[11] Heterogenous base solid catalysts have been developed and successfully applied in the transesterification process of triglycerides (TGs). For instance, the solid base catalyst (K_2O/CaO–ZnO) was tested in the transesterification of soybean oil, at a reaction temperature of 60 °C, with catalyst loading of 2 wt%, methanol to oil molar ratio = 15 : 1, time 4 h. The incorporation of K_2O on the CaO–ZnO catalyst enhanced catalytic activity to yield a maximum conversion of around 81.08 w/w%, due to increased basicity and surface area.[12] While 97 w/w% of biodiesel production was observed over 6 wt% of CaO/Fe_3O_4@SiO_2 catalyst, at a molar ratio of oil to methanol of 1 : 15, 65 °C; mechanical stirring 500 rpm; time 5 h.[13] CaO powder in the catalysis of crude jatropha oil gave around 95.8.% of fatty acid methyl ester (FAME) using an oil to methanol ratio of 1 : 5.15, temperature 65 °C; stirring rate 500 rpm, over 133 min.[14] The optimum FAME product from soybean oil has been reported as about 90% over the novel Mg/Al/Zn hydrotalcite/SBA-15 catalyst, at a reaction temperature 180–300 °C, reaction time of 2 h, oil to methanol molar ratio in the range of 1 : 5 to 1 : 30.[15]

It should be noted that the empirical relationships based on process modelling are key to optimising biodiesel production parameters. An empirical modelling method that has been used to establish the relationship between experimental variables and observed results is response surface methodology (RSM).[16] This method has been used by many researchers to optimise transesterification process parameters. For instance, Abubakar A. *et al.*,[17] optimized biodiesel reaction conditions using RSM and central composite design (CCD) for Jatropha seed oil with 0.30 g of catalyst and ethanol to oil molar ratio of 12 : 1 at 65 °C for 2 h, FAME yield was 98.32%. Their experimental yield was in good agreement with the predicted yield, with a relatively small percentage error (0.58%).[17]

Also, Zabaruddin N. H. *et al.*[18] applied response surface methodology (RSM) for biodiesel synthesis catalysed by radiation-induced kenaf catalyst in a packed-bed reactor. The radiation-treated kenaf (*Hibiscus cannabinus L.*) was functionalized by trimethylamine and then ion-exchanged into the base form with NaOH. The optimum conditions were 9.81 cm packed bed height, a molar ratio of refined palm oil to ethanol of 1 : 50, and a volumetric flow rate of 0.38 mL min^{-1}. Good agreement between the predicted and actual conversions to fatty acid ethyl ester (FAEE) of 97.29% and 96.87%, were achieved respectively.[18] Garg and Jain used both RSM and artificial neural networks (ANN) for the modelling of yield and process parameters. They reported a significant quadratic regression model with values of R^2 of 0.99 and 0.96 for ANN (92% conversion) and RSM with Box–Behnken experimental design (94% conversion), respectively. Their optimum reaction conditions were methanol to algal oil (20–60% (v/v)), catalyst concentration (0–2 wt%) and reaction time (60–180 min) at a constant temperature of 50 °C.[19]

An extensive literature review was conducted[20] on the advantages and disadvantages of the different methodologies in biodiesel production *via* catalytic transesterification. Catalyst structure, morphology, texture, optimization, and reaction parameters such as temperature, catalyst concentration, reaction time, alcohol to substrate molar ratio, and type of alcohol have a significant influence on catalytic activity in biodiesel production.[20] Despite many studies carried out on heterogeneous solid base catalytic transesterification, there are still a number of drawbacks that hinder industrial application. The drive to decarbonisation means there is a need to develop more economically viable solid base catalysts that require less energy in terms of their process conditions yet still maintain optimal efficacy and lifetime.

In this work, the surface functionalized fibrous polyacrylonitrile (PANF) ion-exchange fibres in the form of a mesh, are adapted to produce a strong base ion-exchanger and explored for the first time for efficacy in transesterification reactions. The surface functionalised PANF ion-exchange mesh was obtained by modification of the cyano-group of PANF with a mixture of hydrazine sulphate and hydroxylamine sulphate to produce a crosslinked polymer containing amidoxime, hydrazine, amide and carboxylate groups.[21] This modified PAN was then treated with acid followed by alklali to obtain the strong base catalyst. The main novelty of the present work is the production of protonated and crosslinked hydrazine groups acting as a strong base PANF catalyst and its subsequent use in the transesterification process together with optimization of the experimental parameters, such as temperature, the molar ratio between tristearin (TS) or glycerol mono stearate (GMS) and alcohol, catalyst amount, reaction time, and reusability of catalyst.

2 Experimental

2.1 Chemical materials

The PAN mesh was modified with dihydrazine sulphate (Aldrich with purity > 98%), and hydroxylamine sulphate (99%, Aldrich). The functionalised PANF mesh was acidified using hydrochloric acid (37%, Aldrich) and basified with potassium hydroxide (KOH) (97% Aldrich).

Triglyceride (TG): tristearin-TS, composed of 56.4% stearic acid and 41.3% palmitic acid (Technical grade, Aldrich), glycerol monostearate-GMS, composed of 95.4% monoglycerides (mainly monostearate and monopalmitate), 0.4% free glycerin, 0.5% free fatty acid (Purified, Fisher Scientific). Methyl ester of fatty acid: methyl palmitate (95%, Fisher Scientific), methyl stearate (99%, Fischer Scientific). Toluene (≥99.7% GC), methanol (99.8% GC), dichloromethane (≥99.9%, GC), hexane (95% *n*-Hexane, Fisher Scientific), chloroform-D (99.8% + 0.05% TMS, Goss Scientific Instruments Ltd).

2.2 Preparation of the surface functionalized PANF mesh

The surface functionalized PANF mesh is made on an industrial scale, though it is not currently commercially available and is prepared by modification of the cyano-group of the PANF.[21] Modification solutions were prepared from alkaline hydrazine sulphate and hydroxylamine sulphate at pH 9.5 and heated at 95 °C the PAN mesh for two hours. It was then treated with alkali at pH 12 at 60 °C for 15 minutes followed by washing with water and then drying. The surface functionalized PANF mesh contains approximately 50% PAN yarn and 50% polypropylene. Initially the PANF mesh was used as this was produced in a strongly alkaline environment, however it was found not to work in the transesterification reaction. This surface functionalised PANF mesh was then acidified at ambient temperature for 24 h with 2 M HCl to protonate NH groups such as the substituted hydrazine groups and then dried. This was followed by ion-exchange of Cl^- with OH^- by contact with 2 M NaOH at ambient temperature for 24 h under stirring and dried at ambient temperature for 24 h.

2.3 Transesterification reaction

Transesterification of the model triglyceride (TG) tristearin (TS) and the model mono glyceride (MG) glycol monostearate (GMS) with methanol was carried out in a Radley carousel (see Chart 1) fitted with water reflux condenser. TG or GMS (1 g) and methanol were preheated and then mixed and magnetically stirred under reflux, at a temperature of 65 °C. Then the desired amount of basified catalytic PANF mesh was added to the reactor. To determine the effect of different process parameters, the reaction time, amount of catalyst, and temperature were varied. The catalyst lifetime was also studied by its re-use in fresh feed after each reaction. Most of the transesterification reactions were repeated twice with 0.2–10% error in the % conversion, whilst the average of the reactions was used to plot the results in the Figures below. The total volume of the reaction mixture was in the range of 107.6–109.52 mL to reduce error percentage below 10% on the removal of 1 mL of sample for analysis at each time point resulting in a total removal of 7 mL over the 180 min of the transesterification reaction.

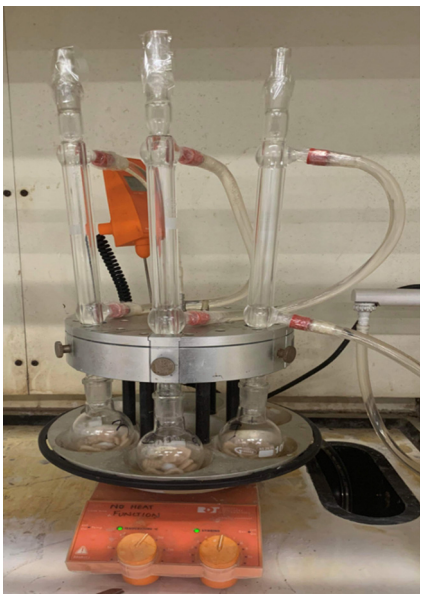

Chart 1 Transesterification reaction under water-cooled reflux in Radley Carousel reactor.

To determine the yield of the methyl ester product the methanol was evaporated from the final transesterification reaction and the FAME product was collected and redissolved in 5 up to 10 mL toluene and injected into the GC-FID. The products of the transesterification of tristearin (TS) and glycerol monostearate (GMS) are methyl stearate (MS) and methyl palmitate (MP), and both MP and MS conversion percentages have been calculated *via* GC-FID areas and with the total conversion labelled as FAME for all samples.

To confirm the production of the esters ^{1}H-NMR was used. After analysis by GC-FID 1 mL of sample product from the transesterification reaction, was taken and dried in an oven at 80–100 °C to remove the toluene solvent used for redissolution and the final product methyl ester was collected and redissolved in chloroform (chloroform-D 99.8% + 0.05%) for ^{1}H-NMR measurements.

2.4 Experimental design of the transesterification reaction

Response surface methodology (RSM) with central composite design (CCD) was used to model the optimum biodiesel production from tristearin (TS). Three independent parameters were evaluated (reaction time, catalyst loading and methanol to TS molar ratio), whilst the dependent variable was the conversion to the fatty acid methyl ester (FAME). The range and levels of the independent variables for the transesterification process are shown in Table 6.

20 sets of experiments were carried out including the 23 factorial experiments, 6 axial points and 6 replicates of centre points as suggested by RSM, (see Table 7 and Section 3.4). The centre points are all variables at level zero which are vital in

determining the level of experimental error and data reproducibility.[45] The transesterification reactions for these twenty experiments comprised different amounts of tristearin in 13 mL of methanol. After the reaction was completed, the PANF catalyst was removed from the solution phase. The reaction mixture was slowly evaporated for 1–2 h at 80–100 °C to evaporate the excess methanol and water. After cooling to room temperature, the methyl ester product and unreacted TG were measured by GC-FID.

2.5 Model fitting and statical analysis

Design Expert software version 13 (STAT-EASE Inc., statistic made easy) was utilised for regression analysis of the experimental data (20 sets of experimental data as described in Section 3.4). The accuracy of the fitted model was determined from the value of correlation (R^2), while the evaluation of the statistical significance of the equations developed was determined using an analysis of variance (ANOVA).[45]

2.6 Methyl stearate (MS)/methyl palmitate (MP) standard solution preparation

Quantitative analysis of the fatty acid methyl esters was performed by GC-FID using calibration curves. The concentrations of the standard fatty acid methyl esters were chosen as between 78 and 2500 ppm with the calibration curves consisting of six concentrations. Triplicate injections were performed for each standard solution for reproducibility. The correlation coefficient was no less than $r^2 = 0.999$, thus confirming the linearity of the method.

2.7 Characterization techniques

GC-FID analysis was conducted in a Thermofisher GC (TRACE1310), equipped with a flame ionization detector (FID) and manual sampler. Sample aliquots of 1 μl were injected using a spilt mode of (40 : 1) with both the injector and detector temperatures held at 250 °C. Hydrogen was used as carrier gas at constant flow (2.4 mL min^{-1}). Chromatographic separation was performed using a nitro-terephthalic acid-modified polyethene glycol capillary column (Zebron ZB-FFAP, GC Cap. Column (60 m × 0.25 mm × 0.25 μm). The oven temperature was set at 200 °C and increased at a rate of 4 °C min^{-1} up to 260 °C. Standards and samples were measured with three triplicates.

^{1}H NMR analyses were conducted using a JEOL ECZ 600 MHz spectrometer operating at 200–300 MHz. The solvent used was deuterated chloroform $CDCl_3$ (chloroform-D 99.8% + 0.05% TMS). Chemical shifts (δ) were expressed in parts per million (ppm), and the values of the coupling constant (J) were expressed in Hertz (Hz). Conversion percentage (C, %), by ^{1}H NMR, was calculated according to eqn (1) given in the literature.[22]

FTIR characterisation of PANF and its basified and regenerated analogues was performed using an ATR-FT-IR (Bruker Alpha Platinum ATR-FTIR) in the range 400–4000 cm^{-1}. Spectra were produced in triplicate using 160 scans and a resolution of 4 cm^{-1}. The following method of data manipulation was also used: Baseline correction, spectrum scaling and smoothing (2 × 25 smoothing points) and a final baseline correction and scaling.[23]

3. Results and discussion

The work in this paper is presented in two parts. Part one is to find values of the process parameters which will be reasonably close enough to the optimum values so as to produce meaningful answers in the DoE simulation.

Thus part one, describes the batch transesterifications of tristearin (TS) and glycerol monostearate (GMS) with methanol by the basified PANF mesh catalyst. The reaction parameters (reaction temperature, amount of catalyst, reactant molar ratio, and reusability and regeneration of the catalyst) were optimized in the single variation method in laboratory-based experiments and the results presented in Section 3.1 up to Section 3.3 and Tables 2 and 3. In part two, a design of experiment (DoE) was performed to determine optimized reaction parameters for transesterification tristearin (TS) only. Here, the reaction temperature was kept constant at 65 °C as this was found to be optimum from the single variation method experiments given in Tables 2 and 3. 20 experiments were carried out using different values of the process parameters from those used in Tables 2 and 3, including 23 factorial experiments, 6 axial points, and 6 replicates of centre points. Central composite design (CCD) was utilized and the three process parameters considered were methanol to TS molar ratio (143–250), catalyst amount (1–2.5 g), and reaction time (60–150 min) at a constant temperature of 65 °C (see Table 6). The results are presented in Sections 3.4.1, 3.4.2 and 3.4.3.

3.1 Qualitative analysis of FAME product by NMR

The ^{1}H NMR spectra of the model compounds tristearin (TS) and methyl ester (FAME) used in this work are shown in Fig. 1a and b. The ^{1}H NMR spectra for the transesterification products of samples FAME-MR 571.1 : 1 and FAME-MR 285.5 : 1 (see Table 1) are shown in Fig. 2a and b. The products of the transesterification reaction of tristearin are methyl stearate (MS) and methyl palmitate (MP) and whilst the yields of MP and MS have been calculated individually *via* GC-FID with the total conversion labelled as FAME, the ^{1}H NMR was found to be unable to easily differentiate between MS and MP. Table 1 summarizes the groups and their chemical shifts. The high intensity of the singlet signal (A) of the $-CH_3$ group of the methyl ester occurs at 3.50 and 3.70 ppm and is clearly present at 3.60–3.7 ppm for the model methyl ester (Fig. 1b) and for the two transesterification products (see Fig. 2a and b),[22] but is clearly absent for tristearin (TS) (see Fig. 1a). This signal will increase with the extent of conversion of tristearin to ester and was found to increase on decreasing the molar ratio of methanol to TS from 571.1 : 1 (FAME-MR 571.1 : 1) to 285.5 : 1 (FAME-MR 285.5 : 1). The triplet signal (B) at 2.24–2.29 ppm of the CH_2 group adjacent to the carbonyl group in tristearin (TS) (see Fig. 1a) occurs at a slightly higher chemical shift (δ) value than that of methyl stearate because of greater deshielding by the

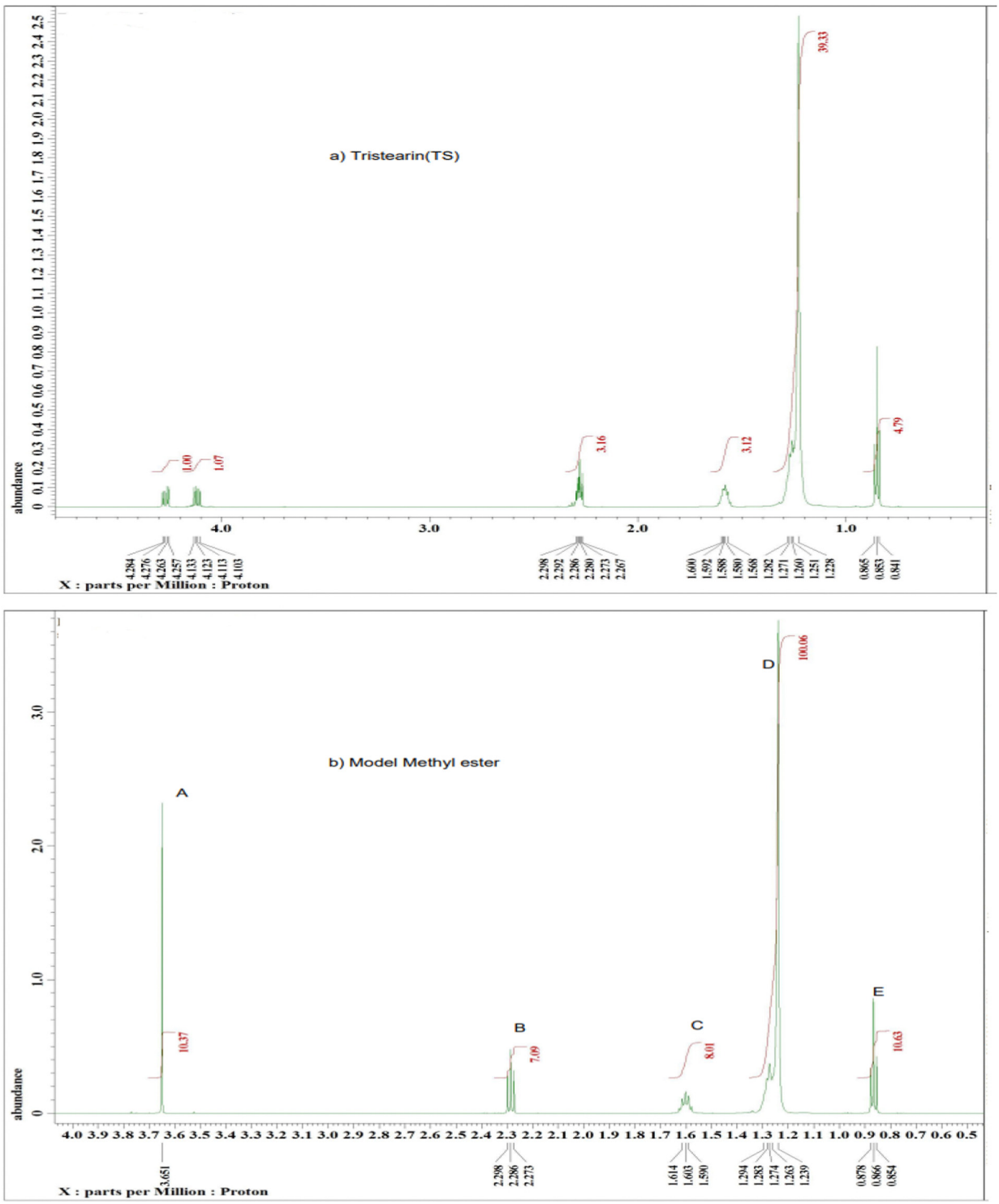

Fig. 1 A typical ^{1}H NMR spectrum of the model compounds (a) tristearin and (b) methyl stearate with labelling of the major peaks.

Table 1 Molecular moieties of methyl esters and their ^{1}H NMR chemical shifts[22,23]

Signal	Moieties	Chemical shifts (ppm)
A	Methyl ester $-CH_3$	3.50–3.70
B	$-CH_2$-adjacent to the carbonyl group	2.24–2.29
C	The aliphatic $-CH_2-$s: CH_2 group is one group away from the carbonyl group.	1.61–1.28
D	$-CH_2$ – in CH_2R: CH_2 groups between the end CH_3 group and the CH_2 group	1.23–1.29
E	End of chain aliphatic $-CH_3$	0.85–0.87

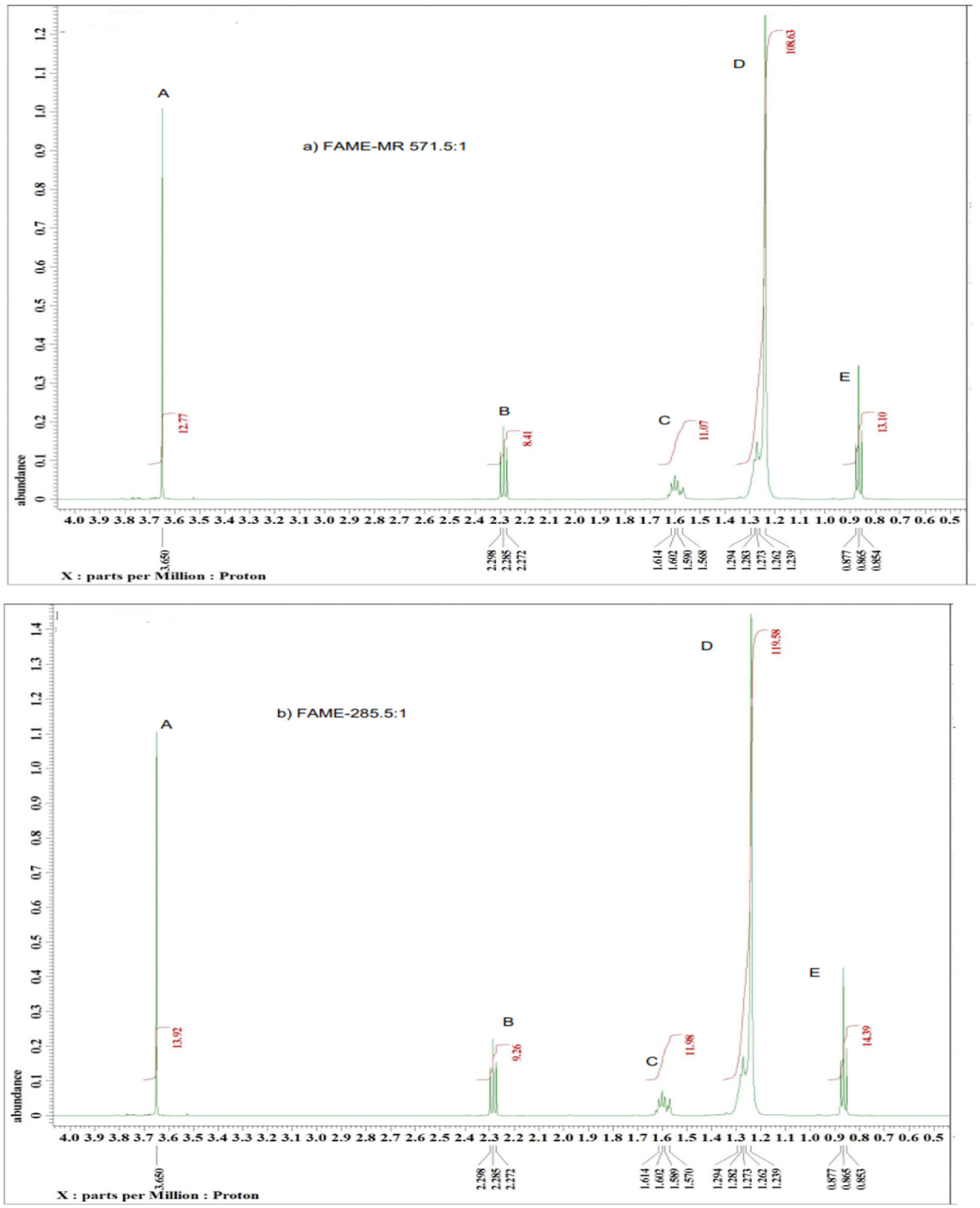

Fig. 2 A typical ^{1}H NMR spectrum of sample (a) FAME-MR 571.5 : 1 and (b) FAME-MR 285.5 : 1 with labelling of the major peaks, reaction conditions: reaction temperature 65 °C, 2 h and over 1.5 g of basified PANF fibrous solid catalyst.

carbonyl group of tristearin (TS) as compared to the ester group (Fig. 1b). The intensity and overall area of the triplet peak (B) of tristearin (TS) decreases which clearly indicates higher conversion of tristearin to methyl ester (see Fig. 2a and b).

3.2 Effect of individual process parameters over basified PANF solid catalyst

As triglycerides and alcohol are immiscible, this limits the surface area available for transesterification and thus slows

the reaction rate.[24] Thus, a solid catalyst can increase the contact between reactants and improve the reaction rate.[24] Thus, the transesterification process is limited by low conversion and a need for long reaction times with several approaches developed to avoid equilibrium establishment and to improve overall conversion and rate of reaction, with significant differences existing between current industrial practices and optimum transesterification processes/conditions. In the following section, tristearin (TS) glycerol monostearate (GMS) has been transesterified *via* solid base PANF fibrous catalyst mesh at moderate reaction temperatures.

3.2.1 Effect of molar ratio of methanol to TS and GMS. The molar ratio of alcohol to oil is an important factor in the production of biodiesel. As noted in the literature,[25] "the reaction stoichiometry requires three moles of alcohol per mole of triglyceride to yield three moles of fatty esters and one mole of glycerine". But in practice, a higher alcohol/oil ratio is usually required to obtain a higher conversion.[26,27] The methanol/oil ratio is one of the most influential factors on reaction rate and conversion, and its optimum value is usually related to the type of catalyst used, among other reaction conditions (type of reactor, temperature, *etc.*).[28,29] However, due to an increase in solubility, the separation of the glycerine product is impeded by the high molar ratio.[29]

Methanol to TS molar ratios were varied from 142.9 : 1 to 571.5 : 1, keeping the remaining parameters constant, as illustrated in Fig. 3a and Table 2. At a lower methanol to TS molar ratio of 142.1 : 1, the conversion to FAME was 47.64% based on GC-FID analysis, which increased to 74.05% and 73.17% on increasing the methanol to tristearin molar ratios to 190.5 : 1 and 285.5 : 1, respectively, as the excess methanol helps to move the transesterification reaction in the forward direction. By further increasing the methanol to TS ratio to 571.5 : 1, the conversion to FAME decreased to 61.48%, due to a dilution effect. This can be explained as follows: the OH^- anion and produced methoxy anion (CH_3O^-) are electrostatically held towards the protonated hydrazine groups on the mesh. Thus, it is likely that the dissolved TS and GMS need to approach closely to the mesh in order to undergo the transesterification reaction. As the solution becomes more dilute the probability of these molecules being found in the vicinity of the mesh decreases. Too much methanol could also hinder the separation of products, thus affecting the final yield of biodiesel. This was probably because the solubility of glycerol in the media increased as the amount of alcohol increased, making it difficult to separate glycerol out from the methyl ester mixture. Therefore, some glycerol remained in the solution and it reduced the conversion of the triglyceride by increasing the back reaction.[30–32]

Fig. 3b and Table 3 show the lowest conversion, 59.83%, of glycerol monostearate (GMS) to FAME at high methanol to GMS molar ratio of 230 : 1. Conversion sharply increased to 80% with decreasing molar ratio of methanol to GMS of 115 : 1, with negligible further increase in conversion from 80% to 83% as the ratio decreased further (see Table 3 and Fig. 3b). Thus, regardless of the mechanism (Rideal or Langmuir–Hinshelwood), both imply that excess methanol adsorption on the catalyst surface results in poorer conversion. Considering these results, going forward the methanol/tristearin ratio of 285.5 : 1, and methanol/GMS molar ratio of 115 : 1 was selected for further study.

Whilst conversion to FAME (biodiesel) was in the range of 80% to 83% for glycerol monostearate (GMS) as compared with 73.17 and 74.47% for tristearin (TS), the optimum methanol molar ratios were different. Not unexpectedly the three backbones of TS needed at least double the amount of methanol than is required for GMS to obtain good conversion to the methyl ester (biodiesel) under the same reaction conditions.

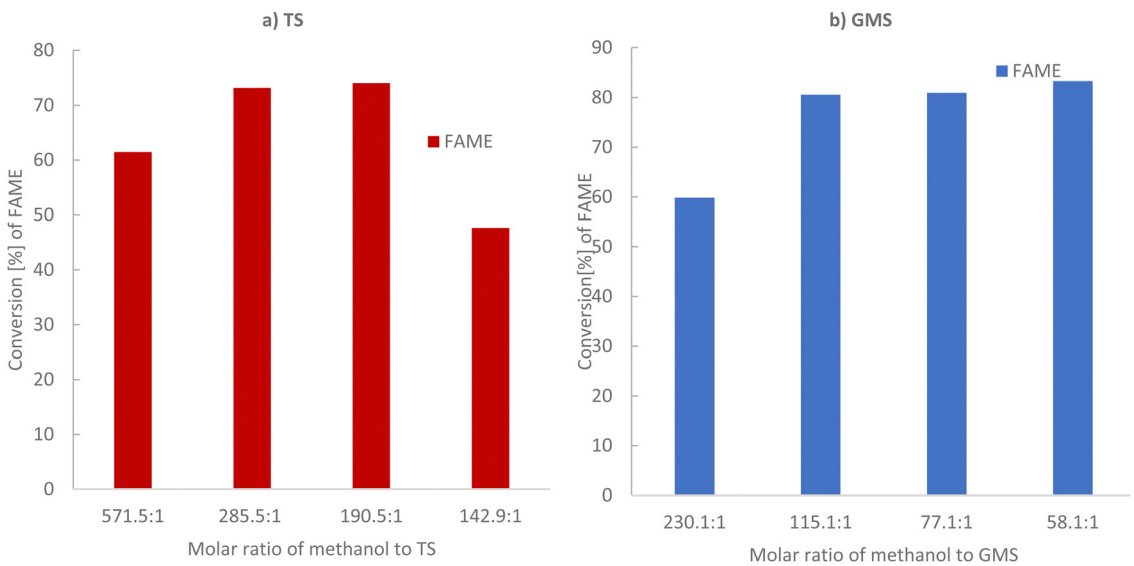

Fig. 3 GC-FID analysis for conversion of triglyceride tristearin (TS) and monoglyceride glycerol monostearate (GMS) to (FAME) as a function of their molar ratio. (a) Tristearin (TS) conversion and (b) GMS conversion. Reaction conditions: 65 °C, 2 h, 1.5 g of solid base PANF catalyst.

Table 2 % conversion of tristearin (TS) to FAMEs with base solid PANF catalyst as analysed by GC-FID

Sample	MR	% conversion to MS ± SD (GC error%)	% conversion to MP ± SD (GC error%)	Total % conversion to FAME ± SD (Batch error%)
Effect of molar ratio of methanol to TS (MR), 65 °C, 1.5 g cat,2 h, volume = 108.95 mL				
FAME-MR 571.5 : 1	571.5 : 1	26.77 ± 0.018	34.71 ± 0.019	61.48 ± 2.30
FAME-MR 285.6 : 1	285 : 6:1	30.61 ± 0.03	42.56 ± 0.01	73.17 ± 1.43
FAME-MR 190.5 : 1	190.5 : 1	30.98 ± 0.042	43.07 ± 0.06	74.05 ± 3.56
FAME-MR 142.9 : 1	142.9 : 1	19.87 ± 0.003	27.77 ± 0.007	47.64 ± 4.76

Samples	Time (min)	% conversion to MS ± SD (GC error%)	% conversion to MP ± SD (GC error%)	Total % conversion to FAME ± SD (bach error %)
Effect of catalyst amount, constant MR = 285.5 : 1, 65 °C, 2.5 g of catalyst volume = 108.95 mL				
FAME-15min	15	5.64 ± 0.035	6.003 ± 0.018	11.643 ± 4.30
FAME-30min	30	8.68 ± 0.017	9.83 ± 0.016	18.51 ± 6.01
FAME-60min	60	13.53 ± 0.008	18.09 ± 0.006	31.62 ± 2.56
FAME-90min	90	15.8 ± 0.123	26.88 ± 0.041	42.68 ± 7.056
FAME-120min	120	29.32 ± 0.0052	40.89 ± 0.012	70.21 ± 3.33
FAME-150min	150	30.38 ± 0.058	45.95 ± 0.005	76.33 ± 4.24
FAME-180min	180	37.96 ± 0.012	51.54 ± 0.021	89.5 ± 5.01
Effect of catalyst amount, constant MR = 285.5 : 1, 65 °C, 4 g of catalyst volume = 108.95 mL				
FAME-15min	15	9.1 ± 0.021	14.54 ± 0.018	23.64 ± 5.30
FAME-30min	30	13.5 ± 0.008	17.98 ± 0.0060	31.48 ± 3.456
FAME-60min	60	17.66 ± 0.047	27.03 ± 0.0052	44.69 ± 2.30
FAME-90min	90	32.87 ± 0.11	46.47 ± 0.0033	79.34 ± 4.56
FAME-120min	120	41.54 ± 0.006	54.08 ± 0.016	95.62 ± 3.67
FAME-150min	150	34.34 ± 0.05	56.03 ± 0.12	90.37 ± 2.23
FAME-180min	180	33.88 ± 0.1	56.56 ± 0.012	90.44 ± 3.89
Effect of catalyst amount, constant MR = 285.5 : 1, 65 °C, 6 g of catalyst volume = 108.95 mL				
FAME-15min	15	25.4 ± 0.012	38.5 ± 0.013	63.9 ± 6.34
FAME-30min	30	25.87 ± 0.003	40.75 ± 0.015	66.62 ± 2.87
FAME-60min	60	32.53 ± 0.05	48.85 ± 0.08	81.38 ± 3.30
FAME-90min	90	41.94 ± 0.008	54.38 ± 0.13	96.32 ± 3.67
FAME-120min	120	37.74 ± 0.006	57.03 ± 0.003	94.77 ± 4.45
FAME-150min	150	34.59 ± 0.006	60.46 ± 0.004	95.05 ± 2.34
FAME-180min	180	35.48 ± 0.12	54.92 ± 0.008	90.4 ± 4.45
Effect of catalyst amount, constant MR = 285.5 : 1, 65 °C, 8 g of catalyst volume = 108.95 mL				
FAME-15min	15	24.97 ± 0.056	41.43 ± 0.014	66.4 ± 2.345
FAME-30min	30	31.43 ± 0.044	44 ± 0.024	75.43 ± 2.67
FAME-60min	60	39.2 ± 0.11	52.26 ± 0.11	91.46 ± 3.567
FAME-90min	90	37.78 ± 0.052	52.97 ± 0.008	90.75 ± 4.30
FAME-120min	120	37 ± 0.019	49.82 ± 0.0034	86.82 ± 4.56
FAME-150min	150	37.58 ± 0.018	49.38 ± 0.13	86.96 ± 1.89
FAME-180min	180	37.56 ± 0.023	51 ± 0.044	88.56 ± 2.30
Effect of reaction temperature, constant MR = 285.5 : 1, 6 g of catalyst, 55 °C volume = 108.95 mL				
FAME-15min	15	15.52 ± 0.12	28.27 ± 0.033	43.79 ± 5.60
FAME-30min	30	23.52 ± 0.022	32.94 ± 0.107	56.46 ± 4.30
FAME-60min	60	28.53 ± 0.031	40.8 ± 0.071	69.33 ± 7.30
FAME-90min	90	32.24 ± 0.017	42.96 ± 0.12	75.2 ± 2.67
FAME-120min	120	34.5 ± 0.11	47.36 ± 0.14	81.86 ± 2.98
FAME-150min	150	35.4 ± 0.056	49.19 ± 0.013	84.59 ± 4.05
FAME-180min	180	35.35 ± 0.068	50.78 ± 0.008	86.13 ± 2.78
Effect of reaction temperature, constant MR = 285.5 : 1, 6 of catalyst, 45 °C volume = 108.95 mL				
FAME-15min	15	4.3 ± 0.02	4.76 ± 0.076	9.06 ± 3.30
FAME-30min	30	6.35 ± 0.05	8.35 ± 0.002	14.7 ± 5.670
FAME-60min	60	13.35 ± 0.04	19.97 ± 0.07	33.32 ± 4.00
FAME-90min	90	22.28 ± 0.05	29.11 ± 0.03	51.39 ± 3.80
FAME-120min	120	23.89 ± 0.07	36.82 ± 0.019	60.71 ± 2.45
FAME-150min	150	33.79 ± 0.038	37.2 ± 0.21	70.99 ± 6.56
FAME-180min	180	37.26 ± 0.17	38.41 ± 0.23	75.67 ± 3.45
FAME-210min	210	36.27 ± 0.003	44.96 ± 0.066	81.23 ± 8.30
FAME-240min	240	43.27 ± 0.16	37.026 ± 0.026	80.296 ± 5.078

Samples	Run no	% conversion to MS ± SD (GC error%)	% conversion to MP ± SD (GC error%)	Total % conversion to FAME ± SD (Batch error%)
Reusability of basified PAN solid catalyst (3 g), 65 °C, MR = 274.8 : 1, 2 h, total vol. 27.33 mL				
FAME-R1	1	45.06 ± 0.063	51.25 ± 0.029	96.31 ± 2.05

Table 2 (*continued*)

Samples	Run no	% conversion to MS ± SD (GC error%)	% conversion to MP ± SD (GC error%)	Total % conversion to FAME ± SD (Batch error%)
FAME-R2	2	44.42 ± 0.056	50.91 ± 0.0072	95.33 ± 3.078
FAME-R3	3	45.78 ± 0.0058	50.64 ± 0.0078	95.42 ± 4.65
FAME-R4	4	39.05 ± 0.011	49.67 ± 0.0076	88.72 ± 3.34
FAME-R5	5	33.16 ± 0.058	49.16 ± 0.0058	82.32 ± 5.08
FAME-R6	6	27.17 ± 0.093	43.64 ± 0.0082	70.81 ± 5.66
FAME-R7	7	29.39 ± 0.017	40.08 ± 0.082	69.47 ± 3.48
FAME-R8	8	19.89 ± 0.026	26.84 ± 0.011	46.73 ± 5.98
FAME-R9	9	14.56 ± 0.005	20.94 ± 0.047	35.5 ± 3.34

Samples	Run no	% conversion to MS ± SD (GC error%)	% conversion to MP ± SD (GC error%)	Total % conversion to FAME
Reusability of basified PAN solid catalyst (3 g) after regeneration, 65 °C, MR = 274.8 : 1, 2 h, total vol. 27.33 mL				
FAME-R1	1	29.17 ± 0.005	41.63 ± 0.011	70.8
FAME-R2	2	25.2 ± 0.0015	33.23 ± 0.067	58.43
FAME-R3	3	13.73 ± 0.0056	18.45 ± 0.047	32.18
FAME-R4	4	7.082 ± 0.0012	10.5 ± 0.0045	17.582

Note: The products of transesterification of tristearin are methyl stearate (MS) and methyl palmitate (MP). The SD is for triplicate injections of the reaction products on the GC. Peak areas of both MS and MP are used to obtain the total % conversion to FAME.

Effect of catalyst amount. In theory, the more catalyst that is added the more products are produced. Our experiments gave results consistent with theory. The effect of the amount of basified PANF solid base catalyst on the transesterification reaction with a molar ratio of methanol to tristearin 285.5 : 1 and methanol to GMS 115 : 1 at 65 °C as a function of the duration of treatment is shown in Fig. 4a and b, (see Tables 2 and 3). For tristearin there was a significant increase in FAME production on increasing the basified PANF solid catalyst from 2.5 g to 6 g, which did not increase further for 8 g of catalyst.[33] 4 g and 6 g of PANF base solid catalyst, gave high conversions of 95.32 and 96.32% w/w respectively, with 6 g of catalyst reaching optimum conversion at 80 min which was earlier than 4 g of catalyst which took 110 min. The results suggest that a catalyst dosage of 6 g provided enough catalytic sites for the reactants. When the amount of catalyst was in excess, mass transfer between the catalyst and reactants decreased, therefore reducing interactions between them and, ultimately, the FAME content.[34] This effect can also be contributed to by the production of soap *via* an unwanted side reaction which could arise from any trapped NaOH.

A similar trend in FAME production was obtained for glycerol monostearate (GMS) with a significant increase in methyl ester (FAME) production from 1.5 g to 4 g of basified PAN solid catalyst, with high conversions of 92.19% and 97.5%, respectively. FAME production was reduced to 84.9% by increasing the catalyst amount to 5.5 g. This has also been observed in homogeneous transesterification catalysis.[35,36] Thus 6 g and 2.5 g basified PANF solid catalysts were selected for tristearin (TS) and glycerol monostearate (GMS) feedstock, respectively, going forward as higher amounts of catalyst did not significantly increase the reaction rate nor FAME production.

3.2.2 Effect of transesterification reaction temperature. The influence of transesterification reaction temperature for both tristearin (TS) and glycerol monostearate (GMS) are shown in Fig. 5a and b. over the temperature range 45 to 65 °C whilst keeping the remaining parameters constant. There was a strong effect on the duration of the induction period and the reaction rate for tristearin but not for GMS, which for TS decreased as the temperature increased. The induction period could result from two factors: the adsorption stage of the reagents (which is a characteristic of heterogeneous catalysis) and diffusion phenomena between the existing phases in the first stage of the catalytic reaction. Temperature increase resulted in better conversions as was expected as the transesterification reaction has been shown to be endothermic.[33] Also, as the transesterification process *via* heterogeneous catalysis is slower in comparison to homogenous catalysis, the effect of temperature is more noticeable.[33] For tristearin (TS) feedstock the maximum conversion to the methyl ester (FAME) of 95.34%, was achieved only at 65 °C and at 90 min. after which there was no further improvement. For glycerol monostearate (GMS), FAME production was almost similar in the range of (81% to 95.05%) for all three temperatures 45 °C, 55 °C, and 65 °C at 60 min after which there was no improvement (see Table 3).

GMS requires a smaller amount of catalyst (2.5 g) than tristearin and in contrast to tristearin, high FAME production is observed for all reaction temperatures in the range 45 °C up to 65 °C. Glycerol monostearate is easier to transform to FAME product as it needs milder reaction conditions, as compared with the need to break three C–C bonds in the glycerol backbone of tristearin.

3.2.3 Basified PAN catalyst reusability and stability. To investigate the extent of re-use of the catalyst in the transesterification reaction the catalyst was removed, and fresh feed was added to the reactor. The reusability of the basified PAN catalyst was examined for nine reaction cycles under the reaction conditions 65 °C, 2 h, and 3 g of base PAN mesh catalyst with a molar ratio of methanol to TS 274.8 : 1, total vol. 27.34 mL. as shown in Fig. 6. It was found that the catalyst maintained high catalytic activity for the first 6 cycles with conversion to the esters ranging from 95–82%, showing good

Table 3 % conversion of glycerol monostearate (GMS) to FAMEs with base solid catalyst as analysed by GC-FID

Samples	MR	% conversion to MS ± SD (GC error%)	% conversion to MP ± SD (GC error%)	Total % conversion to FAME ± SD (batch error%)
Effect of molar ratio methanol to GMS (MR), 65 °C, 1.5 g cat, 2 h				
FAME-MR230 : 1	230 : 1	33.21 ± 0.05	26.62 ± 0.012	59.83 ± 3.45
FAME-MR115 : 1	115 : 1	45 ± 0.035	35.58 ± 0.059	80.58 ± 2.078
FAME-MR 77 : 1	77 : 1	45.13 ± 0.043	35.8 ± 0.025	80.93 ± 6.68
FAME-MR 58 : 1	58 : 1	42.1 ± 0.077	41.28 ± 0.10	83.58 ± 3.38

Samples	Time (min)	% conversion to MS ± SD (GC error%)	% conversion to MP ± SD (GC error%)	Total % conversion to FAME ± SD (batch error%)
Effect of catalyst amount, constant MR = 115, 65 °C, 1.5 g of catalyst, volume = 107.74 mL				
FAME-5min	5	7.078 ± 0.063	6.8 ± 0.046	13.878 ± 5.56
FAME-15min	15	18.234 ± 0.07	12.97 ± 0.078	31.204 ± 3.078
FAME-30min	30	21.6 ± 0.015	18.81 ± 0.026	40.41 ± 5.03
FAME-40min	40	30.53 ± 0.036	28.11 ± 0.004	58.64 ± 4.45
FAME-60min	60	31.28 ± 0.08	37.63 ± 0.04	68.91 ± 2.78
FAME-90min	90	36.21 ± 0.007	34.89 ± 0.0062	71.1 ± 3.98
FAME-120min	120	43.82 ± 0.0095	36.14 ± 0.058	79.96 ± 5.00
Effect of catalyst amount, constant MR = 115, 65 °C, 2.5 g of catalyst, volume = 107.74 mL				
FAME-5min	5	26.16 ± 0.05	21.64 ± 0.004	47.8 ± 2.78
FAME-15min	15	36.51 ± 0.09	29.3 ± 0.0014	65.81 ± 4.38
FAME-30min	30	45.08 ± 0.008	35.08 ± 0.036	80.16 ± 5.34
FAME-40min	40	48.4 ± 0.08	39.92 ± 0.006	88.32 ± 3.88
FAME-60min	60	50.1 ± 0.09	47.4 ± 0.056	96.63 ± 2.34
FAME-90min	90	51.08 ± 0.05	44.5 ± 0.008	95.58 ± 3.45
FAME-120min	120	50.09 ± 0.007	40.9 ± 0.06	90.99 ± 56.45
Effect of catalyst amount, constant MR = 115, 65 °C, 4 g of catalyst, volume = 107.74 mL				
FAME-5min	5	31.73 ± 0.07	25.93 ± 0.02	57.66 ± 4.56
FAME-15min	15	40.55 ± 0.021	29.93 ± 0.05	70.01 ± 2.078
FAME-30min	30	40.38 ± 0.01	40.43 ± 0.03	80.81 ± 3.34
FAME-40min	40	42.48 ± 0.04	43.23 ± 0.026	85.71 ± 5.26
FAME-60min	60	47.93 ± 0.06	44.26 ± 0.0028	92.19 ± 4.50
FAME-90min	90	51.03 ± 0.004	39.64 ± 0.025	90.67 ± 2.056
FAME-120min	120	44.33 ± 0.02	45.08 ± 0.008	89.41 ± 4.98
Effect of catalyst amount, constant MR = 115, 65 °C, 5.5 g of catalyst, volume = 107.74 mL				
FAME-5min	5	36.65 ± 0.018	27.9 ± 0.022	64.55 ± 6.54
FAME-15min	15	39.64 ± 0.033	32.13 ± 0.0026	71.77 ± 5.23
FAME-30min	30	41.35 ± 0.089	34.6 ± 0.089	75.95 ± 3.45
FAME-40min	40	46.99 ± 0.035	32.85 ± 0.002	79.84 ± 2.56
FAME-60min	60	45.73 ± 0.044	36.59 ± 0.0026	82.32 ± 4.078
FAME-90min	90	34.22 ± 0.0025	50.68 ± 0.0018	84.9 ± 7.07
FAME-120min	120	55.035 ± 0.094	28.68 ± 0.13	83.72 ± 3.67
Effect of reaction temperature, constant MR = 115, 2.5 of catalyst, 55 °C, volume = 107.74 mL				
FAME-5min	5	21.44 ± 0.097	22.25 ± 0.075	43.69 ± 4.078
FAME-15min	15	26.55 ± 0.044	32.69 ± 0.032	59.24 ± 3.99
FAME-30min	30	43.3 ± 0.023	31.19 ± 0.098	74.69 ± 1.73
FAME-40min	40	47.83 ± 0.049	37.73 ± 0.036	85.56 ± 4.65
FAME-60min	60	50.47 ± 0.050	39.58 ± 0.086	90.05 ± 2.55
FAME-90min	90	50.58 ± 0.15	37.16 ± 0.011	87.74 ± 6.05
FAME-120min	120	47.85 ± 0.089	38.72 ± 0.078	88.57 ± 3.66
Effect of reaction temperature, constant MR = 115, 2.5 of catalyst, 45 °C, volume = 107.74 mL				
FAME-5min	5	21.56 ± 0.09	15.69 ± 0.04	37.25 ± 7.87
FAME-15min	15	32.32 ± 0.011	20.071 ± 0.031	53.391 ± 3.98
FAME-30min	30	35.78 ± 0.12	35.5 ± 0.02	71.28 ± 4.768
FAME-40min	40	40.65 ± 0.071	37.19 ± 0.03	77.84 ± 2.56
FAME-60min	60	44.23 ± 0.05	37.22 ± 0.014	81.45 ± 3.95
FAME-90min	90	43.69 ± 0.03	40.37 ± 0.11	84.06 ± 2.47
FAME-120min	120	42.66 ± 0.025	40.9 ± 0.06	83.56 ± 5.67

The products of transesterification of glycerol monostearate are methyl stearate (MS) and methyl palmitate (MP). The SD is for triplicate injections of the reaction products on the GC. Peak areas of both MS and MP are used to obtain the total % conversion to FAME.

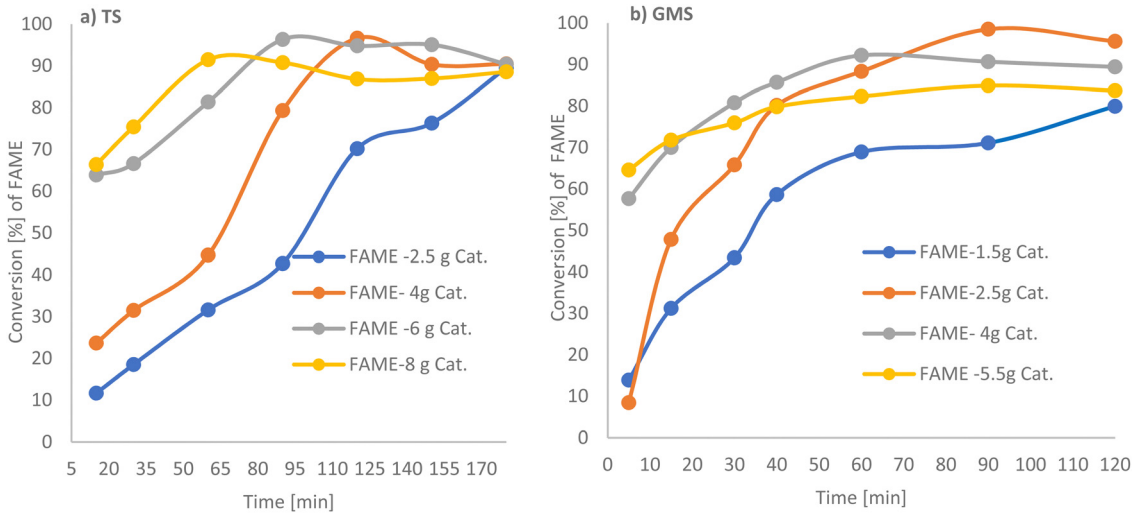

Fig. 4 GC-FID analysis for the conversion of TS and GMS to FAME as a function of solid base PANF catalyst loading. (a) TS to methyl ester for a molar ratio of methanol to TS 285.5 : 1, total vol. 108.95; and (b) GMS to FAME for a molar ratio of methanol to GMS 115.1 : 1, total vol. 107.74 mL, at 65 °C.

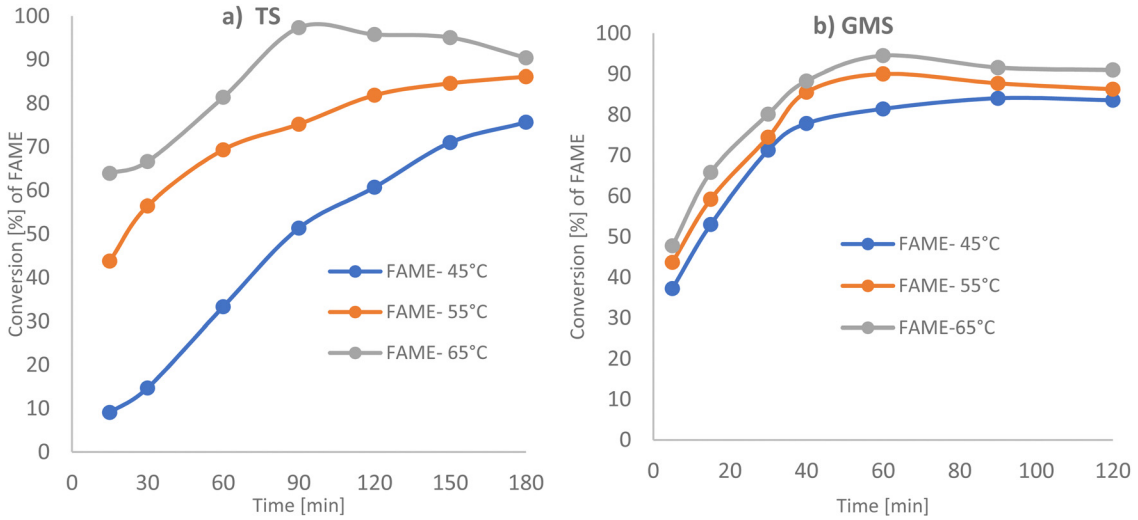

Fig. 5 GC-FID analysis for conversion of TS and GMS to FAME as a function of temperature (a) TS to methyl stearate for the molar ratio of methanol to TS 285.5 : 1, total vol. 108.95 mL, 6 g of PANF base catalyst; (b) GMS to methyl stearate for the molar ratio of methanol to GMS 115.1 : 1, total vol. 107.74 mL, 2.5 g of PANF base catalyst.

stability of the catalyst similar to that obtained by Chumuang *et al.* using the heterogeneous catalyst calcium methoxide.[37] Conversion decreased gradually to 35% for the ninth cycle (see Table 2 and Fig. 6). The reduction in activity after each cycle using the recycled catalyst indicated the deactivation of active sites.[38,39]

To investigate regeneration of the basified PANF solid catalyst for repeated use, the PANF mesh was recovered after the 9th cycle of reaction and washed briefly with dichloromethane (DCM) to dissolve off any adsorbed organic reaction products/reactants. The PANF catalyst was regenerated with 30 mL of 2 M HCl solution for 24 h after which it was immersed in 2 M NaOH for 24 h under stirring and dried for 24 h. Subsequently, the regenerated PANF base catalyst was reused in the transesterification process. The catalytic activity of the regenerated PANF base solid catalyst was regained to give 70–58% conversion of TS to FAME for two more cycles (see Fig. 6 and Table 2). However catalytic activity significantly decreased after the third cycle with conversion reduced to about 17% for the fourth cycle. This suggests that the brief wash with dichloromethane was not sufficient to remove adsorbed compounds (Fig. 6). This is corroborated by the FTIR spectrum of the initial basified PANF catalyst in Fig. 7 and the deactivated and reused catalysts in Fig. 8.

Thus, one of the reasons for the drop in the catalytic activity was the leaching of the hydroxyl ion from the PANF-basified solid catalyst. It could also be due to the blocking of the basic sites of the catalyst. The first cycles after regeneration resulted in a significantly lower conversion to the ester than those of the first cycles before regeneration and unlike the initial cycles,

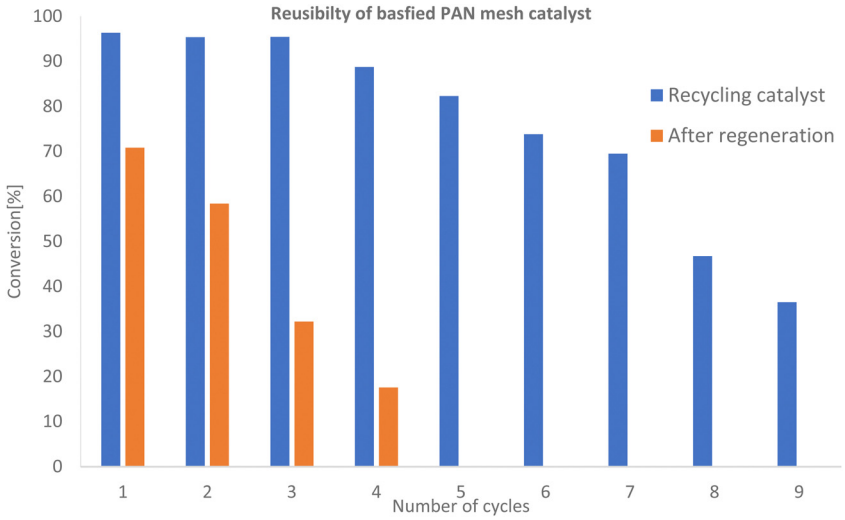

Fig. 6 GC-FID analysis for conversion of tristearin (TS) to FAME as a function of the number of cycles. Reaction conditions: 65 °C, 3 h, 3 g of catalyst, Molar ratio of methanol to TS was 274 : 1, volume = 27.34 mL.

there was a steep drop-in activity. It is possible that in each cycle before regeneration, a significant amount of organic product and byproduct such as the methyl ester product, unreacted tristearin and glycerol was gradually building up and deposited on the fibres of PANF mesh causing deactivation by blocking access to the active sites. It is also possible that all these by-products glycerol, unreacted TGs and the methyl ester could prevent the hydrochloric acid and sodium hydroxide treatment from hydroxylation of the amine groups on the amidoxime functionalized PANF. The regeneration of the base catalyst was then due solely to sodium hydroxide absorbed between the fibrils of the fibrous catalyst, which quickly leached out resulting in its poor performance. However, a more extensive regeneration protocol of the basified PANF catalyst of our work would likely show promise in improving efficacy after regeneration. Thus, further studies about the causes of this deactivation are required to clarify whether blocking of active sites or loss of basicity, among other factors, is responsible.

Nonetheless, our heterogenous basified PANF solid catalyst showed a very high catalytic activity after 9th recycles and for four cycles after regeneration as compared to other works.[40–43]

3.3 FTIR analysis of the basified catalyst and regenerated catalyst

The FTIR assignments of the ion exchange PANF can be found in Table 4 and as indicated in previous papers.[23,44] In short, the groups present on the ion exchange PAN consist of amidoximes (C═N–OH) and hydrazines (C–NH–NH_2) Scheme 1.

Upon acidification with 2 M HCl, there is a significant reduction in the 1512 cm^{-1} peak assigned to NH_2 in amidoximes and hydrazines owing to protonation. There is a reduction in the 920 cm^{-1} N–OH amidoxime peak which is possibly due to a shift to lower wavenumbers upon protonation. There is also evidence in the FT-IR of some acid hydrolysis of the amidoxime group to amides with further hydrolysis to carboxylic acids, which could contribute to the growth of the C═O 1660 cm^{-1} peak and the C–O peak at 1200 cm^{-1}. The presence of carboxylic acid groups will also add OH groups which is demonstrated by the intense and broad peak at 3400–2800 cm^{-1} which centres ~3000 cm^{-1}. Amine salts also adsorb in the 2800–3000 cm^{-1} region which explains the growth of this peak on acidification.

Thus, acidification of PANF resulted in the protonation of the hydrazine groups in both crosslinked and uncrosslinked forms. Hydrazine is a strong base and once protonated it is difficult to deprotonate. These positively charged groups will form electrostatic bonds with the negatively charged chloride ions on acidification which ion-exchange with OH^- during basification with NaOH to form a strong base. It is likely that the OH^- then reacts with the methanol to form the methoxide ion which catalysis the transesterification in the usual manner.

From the stacked spectra in Fig. 7, it is likely that the basification process further converted some amide groups formed during acid hydrolysis to carboxylate groups *via* alkaline hydrolysis. The spectrum of basified PAN in Fig. 7 also shows further reduction of the 920 cm^{-1} N–OH amidoxime group, and the reduction in intensity of the 1626 cm^{-1} C═N group of amidoxime. The re-basification of the ion exchange polymer also reforms the NH_2 groups in amidoxime *via* deprotonation as indicated by the regrowth of the peak at 1512 cm^{-1}. This peak at 1512 cm^{-1} is also assigned to the COO^- peak which is also reformed on de-protonation.

In Fig. 8, the FT-IR spectrum of the deactivated catalyst is stacked alongside the fresh acidified and then basified catalyst and the regenerated catalyst. The deactivated catalyst was very similar to the fresh catalyst except for a few differences which heavily suggest active site blockage. The deactivated catalyst was visibly seen to have a white substance trapped within its fibres which was identified as an ester by FTIR analysis (Fig. 8 and Table 5) with a new low-intensity peak at 1740 cm^{-1} which can be assigned to C═O of an ester. The band at 3000–3400 cm^{-1} has also increased significantly in intensity due to the deposition of the long chain esters adding to the C–H peaks at 2900 cm^{-1}.

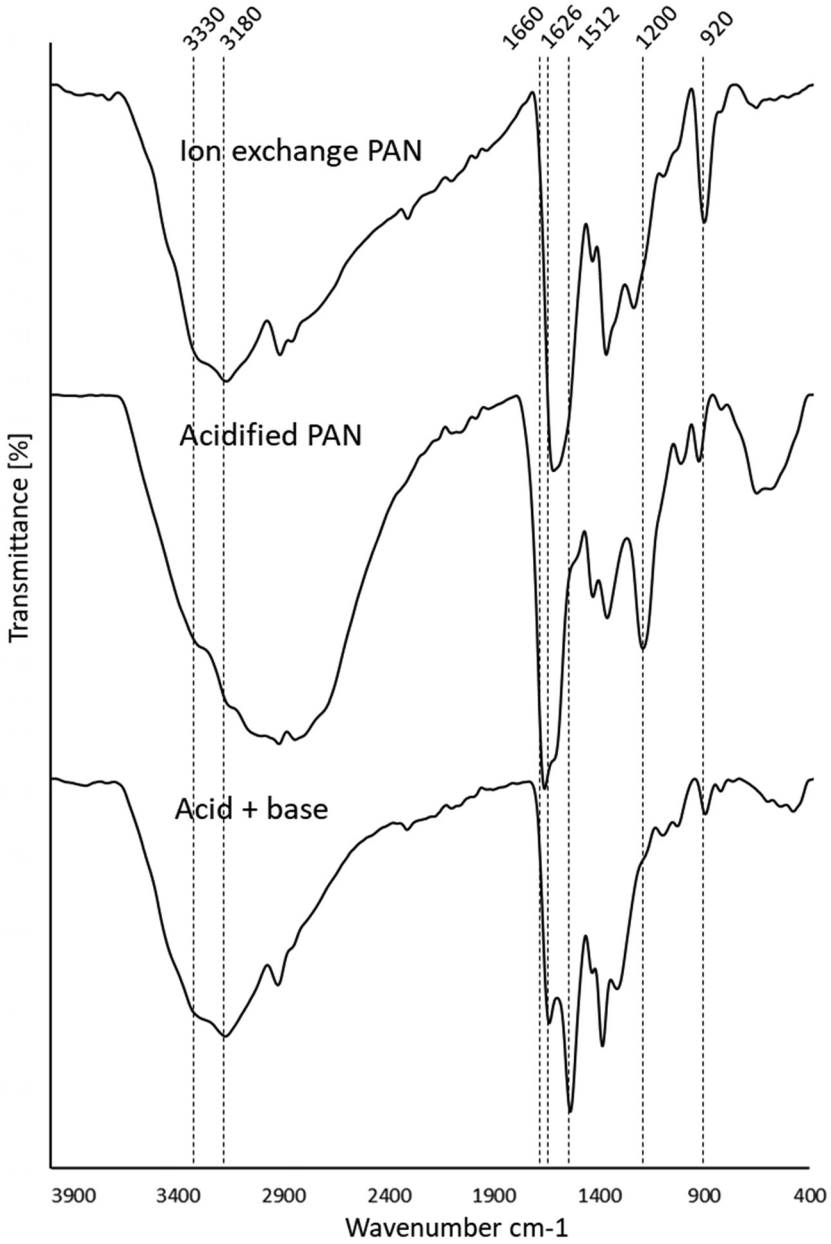

Fig. 7 Stacked FTIR spectra of the ion exchange PANF, the ion exchange PAN in its acidified and basified forms.

Interestingly, both the C═N (1626/1650 cm^{-1}) and NH_2/COO^- (1550 cm^{-1}) peaks do not change in either intensity or position. This indicates that these groups are not affected by deactivation and remain in their basified forms.

The white substance was scraped off the deactivated catalyst, analysed on the FTIR and compared to the spectra of both tristearin and FAME product. As can be seen from Fig. 9, the spectrum of the white substance highly resembles that of tristearin with the positions and intensities of all the peaks identical. The spectrum of the white substance was also compared to the spectra of both methyl stearate and methyl palmitate and whilst the spectra are very similar there are noticeable differences especially in the C–O peaks at 1169 and 1100 cm^{-1} which are very much smaller for methyl stearate and methyl palmitate than for tristearin. The FT-IR of the FAME product also has a low intensity band at 3345 cm^{-1} ascribed to OH, most likely due to the presence of small amounts of mono and/or diglycerides or possibly fatty acid, however the white substance does not have any intensity in this region suggesting that it was unreacted tristearin.

This suggests that the PANF catalyst experienced a continuous loss of OH^- ions over the 9 consecutive transesterification cycles, whereby conversion also decreased leading to a build-up of tristearin on the fibres.

Upon regeneration in Fig. 8, the broad, intense band at 3400–2000 cm^{-1} reduces in intensity, suggesting the loss of NH groups by hydrolysis to OH groups which are generally broader and less intense. The presence of the high-intensity C–H peak

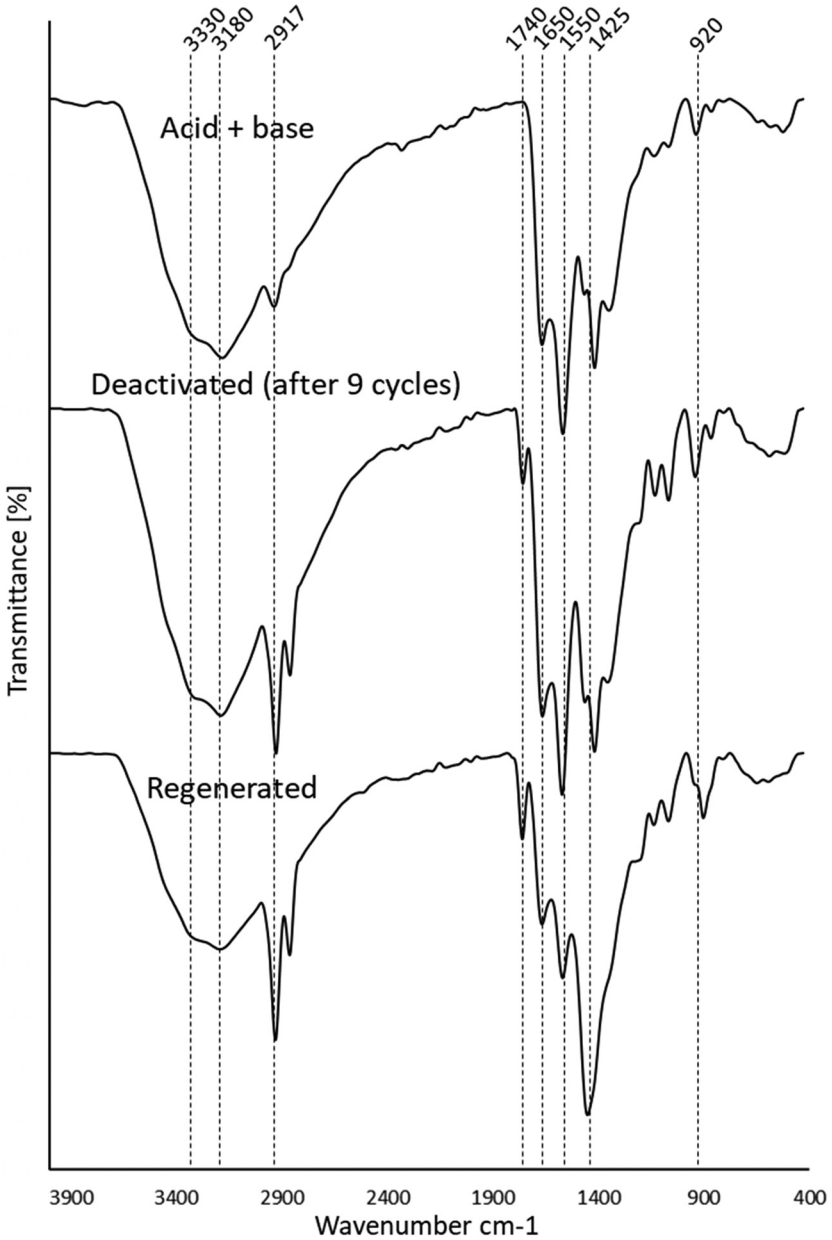

Fig. 8 Stacked FTIR spectra of the basified catalyst, the deactivated and regenerated catalysts.

at 2917 cm^{-1} (also present in the white substance in Fig. 9) suggests that the washing regime with DCM was not sufficient to remove the tristearin (TS) blocking the catalyst active sites. This is further supported by the unchanged intensity of the tristearin C═O peak at 1740 cm^{-1} and the high-intensity CH_2 peak at 1425 cm^{-1}. The C═N (1626 cm^{-1}) and NH_2/COO^- (1550 cm^{-1}) groups have decreased in intensity in comparison to those of the initial acid and then basified catalyst suggesting that there has been a loss of these groups due to hydrolysis on regeneration. There is also the possibility that under the heated basic conditions of the transesterification reaction that the reactants and/or products reacted with the amine and/or carboxylate groups present on the catalyst to form fatty acid amides or fatty acid esters chemically bound to the catalyst, which could then not be washed off. It is difficult to interpret the FT-IR spectrum of the regenerated catalyst to definitively ascribe the mechanism of deactivation on regeneration. However, it seems that regeneration was not effective owing to both loss of sites on regeneration, chemical binding of active sites with reactant/products and blocking of the sites by the tristearin which were not removed by the DCM wash.

3.4 Design of experiment transesterification reaction

In this study, the design of experiment [DoE] was performed as follows: 20 experiments were carried out, including 23 factorial experiments, 6 axial points, and 6 replicates of centre points. Central composite design (CCD) was utilised and the three process parameters considered were methanol to TS molar ratio (143 : 1 to

Table 4 Assignments of the FTIR peaks in Fig. 7

Wavenumber cm^{-1}	Ion exchange PAN fibres	Acidified ion exchange PAN fibres	Acidified and then basified PAN fibres	Assignment[23,44]
3330	X	X	X	OH, amidoxime OH, carboxylic acid
3180	X	X	X	NH, amidoxime, hydrazine and amide
3000–2800		X		NH_2^+ and NH_3^+ amidoxime, hydrazine and amide
1660	X	X	X	C═O amide/imide, carboxylate/carboxylic acid
1626	X	X	X	C═N, amidoxime
1550–1512	X		X	NH_2, amidoxime and hydrazine COO^-, carboxylate
1200	X	X		C–O carboxylic acid
920	X	X	X	N–OH, amidoxime

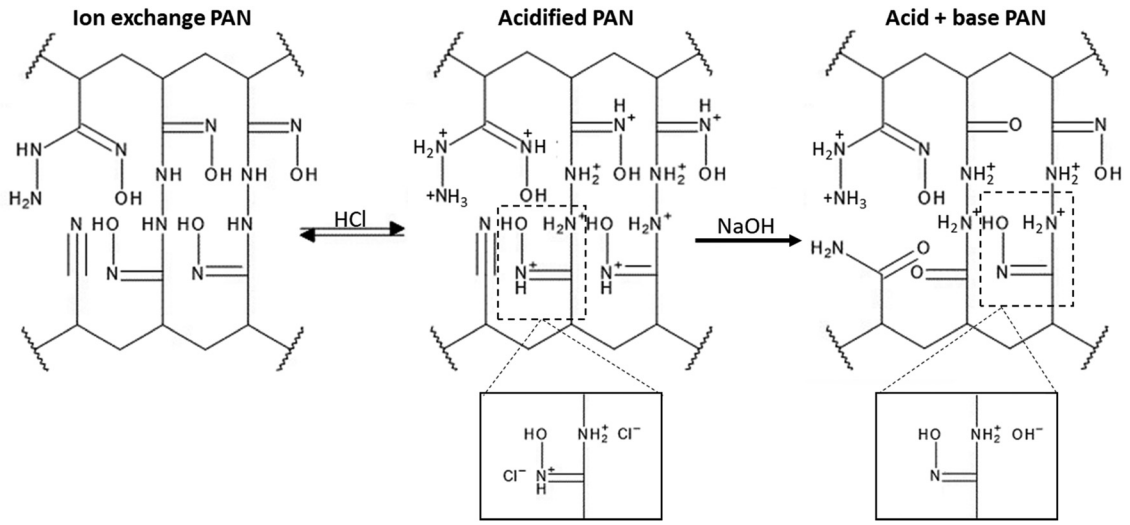

Scheme 1 Structures of the ion exchange PAN upon acidification and subsequent basification (Partially reproduced from Ahmed R.)[23]

Table 5 Assignments of the FTIR peaks in Fig. 8

Wavenumber cm^{-1}	Acidified and then basified PAN fibres	Deactivated PAN fibres	Regenerated PAN fibres	Assignment[23,44]
3330	X	X	X	OH, amidoxime OH, carboxylic acid
3180	X	X	X	NH, amidoxime and hydrazine
2917	X	X	X	C–H, PAN fibres and ester (tristearin)
1740		X	X	C═O, ester (tristearin)
1650		X	X	C═O, amide/imide, carboxylate
1626	X	X	X	C═N, amidoxime
1550	X	X	X	NH_2, amidoxime and amide COO^-, carboxylate
1425	X	X	X	CH_2, PAN fibres and ester (tristearin)
920	X	X	X	N–OH, amidoxime

250 : 1), catalyst amount (1 g to 2.5 g) and reaction time (60 to 150 min) at a constant temperature of 65 °C (see Table 6). These parameters were calculated from the regression formula (eqn (1)).

The batch transesterification reaction experiments were performed for all 20 reaction conditions as given in Table 7 for factors 1, 2 and 3 which are the outcomes of the design of the experiment [DoE] and calculated from the regression formula (eqn (1)). The products of these reactions were measured *via* GC-FID to yield the percentage FAME conversion which was then input (see Table 6) in the design of the experiment to run the DoE.

The results from the experimental transesterification data were fitted to a mathematical model that correlates the FAME conversion with the independent reaction variables *via* a second-order polynomial equation as given below.[45]

$$Y = b_0 \sum_{i=1}^{n} b_i x_i + \sum_{i=1}^{n} b_0 x_i^2 + \sum_{i=1}^{n=1} \sum_{j=i+1}^{n} b_0 x_i x_j \ldots \qquad (1)$$

where Y is the predicted biodiesel yield, b_0 is the constant coefficient, b_i is the linear coefficients, b_{ij} is the interaction

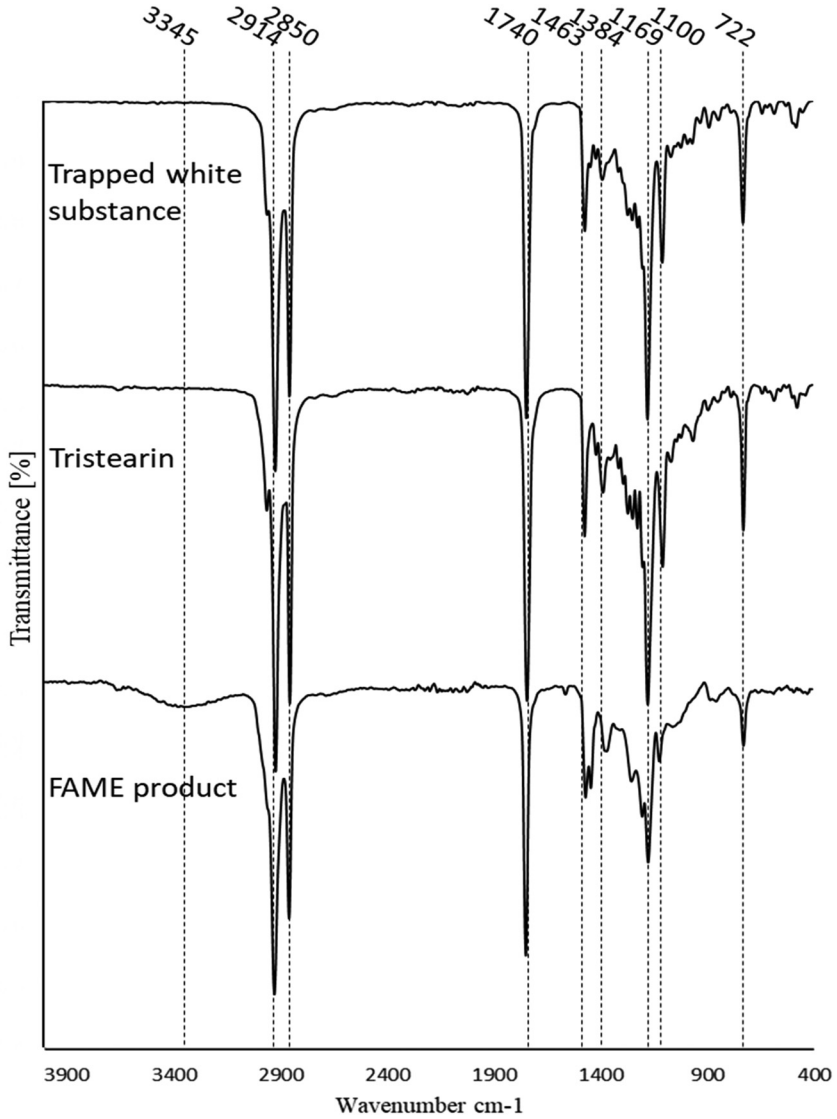

Fig. 9 FTIR spectra of the white substance (esters) in deactivated fibres.

Table 6 The levels and range of the independent variables for the transesterification process

Variables				Levels			
	Coding	Unit	$-\alpha$	-1	0	1	$+\alpha$
Molar ratio	A	Molar	106.524	143	196.5	250	286.476
Catalyst	B	g	0.488655	1	1.75	2.5	3.01134
Time	C	min	29.3293	60	105	150	180.681

coefficients, b_{ii} is the quadratic coefficients and while x_i, x_j are the values of the experimental variables.

3.4.1 Development of experimental regression model. The complete design matrix of experiments together with the experimental and predicted values are shown in Table 7. From Table 7, conversion to FAME is in the range of 36.35% to 87.62%. The RSM software produced a series of models (linear, two-factor reaction (2FI), quadratic and cubic polynomial) that was fitted to the response as well as recommending the best-fitted model as shown in Table 8. According to the sequential model sum of squares, the best model to fit the response is a quadratic owing to its highest order polynomial with the significance of additional terms and the model was not aliased. The final equation in terms of actual factors for biodiesel production was calculated using eqn (2) below.

$$\text{FAME [\%]} = +58.41 - 1.38A + 2.03B - 10.94C - 1.6AC - 88BC - 4.03A^2 + 0.2965B^2 + 2.25C^2 \quad (2)$$

where the terms A, B and C represent the methanol to tristearin molar ratio, catalyst amount, and reaction time, respectively.

Positive signs in front of the terms indicate a synergic effect, while negative sign indicates an antagonistic effect.[46] The terms B, AC, B^2 and C^2 therefore, play an important role in increasing the FAME conversion, whilst the other terms A, C, AB, BC and A^2, play an important role in decreasing the biodiesel concentration.

Table 7 Design of experiments and their respective experimental and predicted value

Runs	Factor 1 A: molar ratio	Factor 2 B: catalyst amount (g)	Factor 3 C: reaction time (min)	Response 1 Experimental value conversion (%)	Response 1 Predicted value conversion (%)
1	250	1	60	50.95	51.18
2	143	1	150	40.64	40.58
3	196.5	0.50	105	55.85	55.83
4	250	1	150	59.23	59.08
5	106.52	1.75	105	49.28	49.33
6	196.5	1.75	105	57.44	58.41
7	286.5	1.75	105	44.75	44.68
8	196.5	1.75	105	58.84	58.41
9	196.5	1.75	105	58.15	58.41
10	250	2.5	150	48.17	48.15
11	196.5	1.75	105	58.37	58.41
12	196.5	1.75	105	59.13	58.41
13	196.5	1.75	105	58.51	58.41
14	196.5	1.75	30	83.46	83.17
15	196.5	3.00	105	62.66	62.66
16	250	2.5	60	63.69	63.76
17	143	2.5	150	36.35	36.14
18	143	2.5	60	87.62	87.79
19	143	1	60	68.69	68.72
20	196.5	1.75	181	46.12	46.39

Table 8 Sequential model sum of squares

Source	Sum of squares	Df	Mean square	*F*-value	*p*-Value	
Mean *vs.* Total	65883.72	1	65883.72			
Linear *vs.* Mean	1716.03	3	572.01	7.10	0.0030	
2FI *vs.* Linear	946.80	3	315.60	12.00	0.0005	
Quadratic *vs.* 2FI	**339.74**	**3**	**113.25**	**554.67**	**<0.0001**	**Suggested**
Cubic *vs.* Quadratic	0.3172	4	0.0793	0.2759	0.8834	Aliased
Residual	1.72	6	0.2874			
Total	68888.33	20	3444.42			
Summary Fit statistic						
Std. Dev.	0.4519		R^2	0.9993		
Mean	57.40		Adjusted R^2	0.9987		
C.V.%	0.7873		Predicted R^2	0.9983		
Std. Dev.	0.4519		Adeq Precision	161.6487		

"Sequential model sum of square": Select the highest order polynomial where the additional terms are significant, and the model is not aliased.

Table 9 Interaction variance effects

Source	Sum of squares	df	Mean square	*F*-Value	*p*-Value	
Model	3002.57	9	333.62	1634.02	<0.0001	Significant
A: molar ratio	26.10	1	26.10	127.82	<0.0001	
B: catalyst amount	56.48	1	56.48	276.63	<0.0001	
C: reaction time	1633.45	1	1633.45	8000.43	<0.0001	
AB	21.00	1	21.00	102.83	<0.0001	
AC	649.44	1	649.44	3180.87	<0.0001	
BC	276.36	1	276.36	1353.57	<0.0001	
A^2	234.26	1	234.26	1147.36	<0.0001	
B^2	1.26	1	1.26	6.18	0.0322	
C^2	73.14	1	73.14	358.24	<0.0001	
Residual	2.04	10	0.2042			
Lack of fit	0.3184	5	0.0637	0.1847	0.9563	Not significant
Pure error	1.72	5	0.3447			
Cor total	3004.61	19				

df = is the degree of freedom [the number of values of a system that varies independently is called degrees of freedom (DF)].

3.4.2 ANOVA analysis. Variance analysis was carried out to establish the effect of different catalysis variables on the conversion efficiency of tristearin into FAME products. The response surface linear model is shown in Table 9. A Model

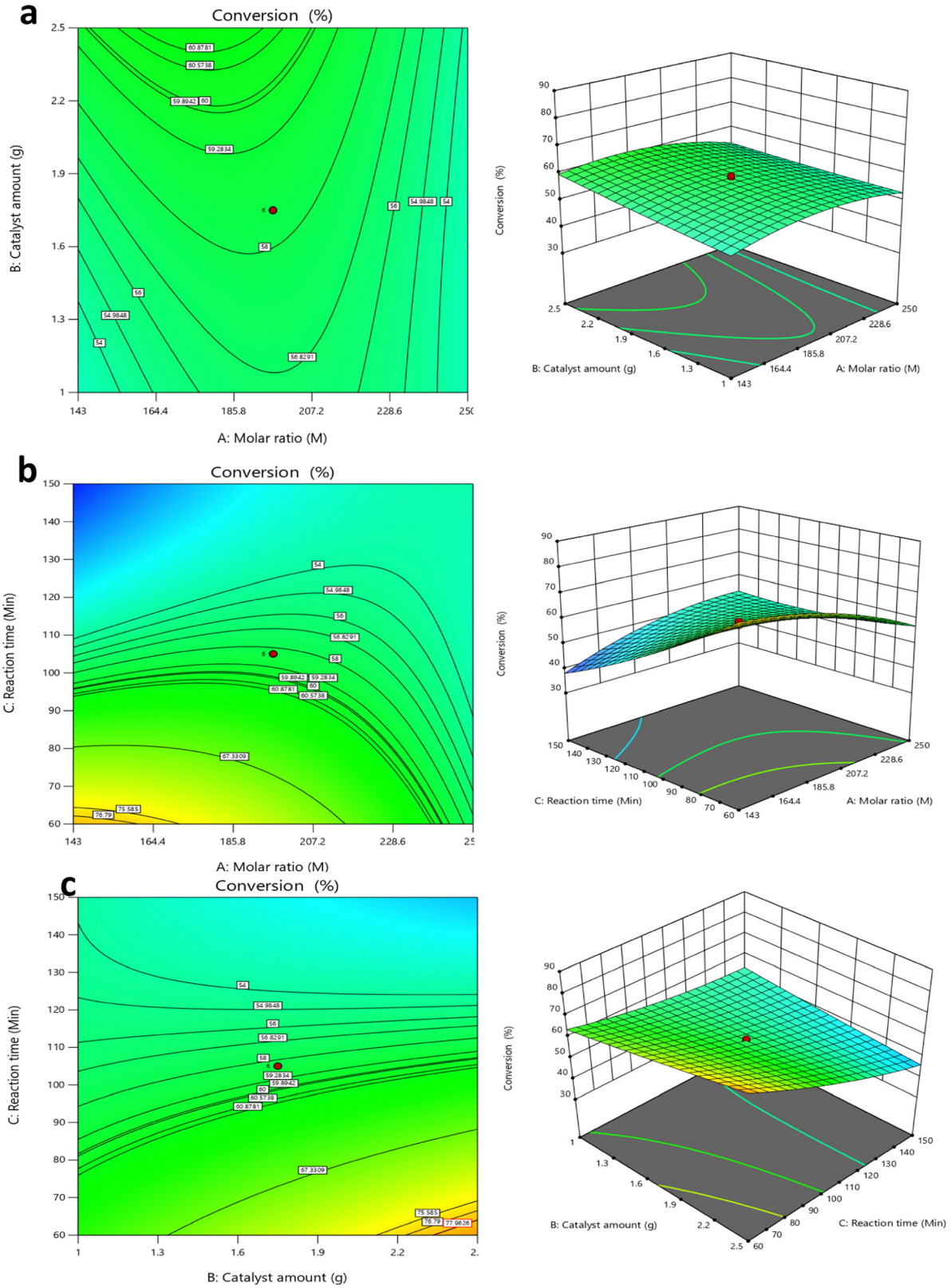

Fig. 10 Contour plot and 3D response curve for conversion of TS to FAME (biodiesel), (a) interaction of catalyst amount and molar ratio, (b) interaction between reaction time and molar ratio and (c) interaction between reaction time and catalyst amount.

F-value of 1634.02 was calculated (see Table 9) indicating that the model is significant. Therefore, the chance that an *F*-value this large could occur due to noise is only 0.01%. Table 9 suggests the parameters with a probability (*P*) value less than

0.05 are significant, and more than 0.1 are considered insignificant.[47] Thus, in this study, the *P* value is less than 0.05 which indicates model terms are significant. In this case, A, B, C, AB, AC, BC, A^2, B^2, and C^2 are significant model terms. The Lack of Fit *F*-value of 0.1847 is insignificant. A lack of fit value similar to this has been attributed to noise as suggested by Zanjani *et al.*, 2013.[47,48]

R^2, adjusted R^2, predicted R^2, C.V., *F* value and *P* values were examined in the model produced by RSM. The significance of the equation was checked by the *F*-test technique. In addition, *P*-values are utilized to verify the importance of each coefficient, which indicates the power of each by-product to interact. The smaller *P* values lead the associated coefficients to be of great importance. An extremely low *P*-value (<0.0001) of the *F* model at a 95 percent confidence level indicates that the regression model is statistically significant. The determination coefficient (R^2) that indicates connections between the actual FAME product and the anticipated product is estimated as 0.9993. Moreover, 0.9987 and 0.9983 respectively are adjusted and projected R^2, with a low standard deviation value, was 0.4519 (see Table 8). These values reveal the fitted model to be outstanding. C.V., which must be less than 10%, is another key element for the evaluation of the model. This model is acceptable for the projected biodiesel produced by tristearin as the C.V. fitting model values are 0.7873%.[49]

3.4.3 Study of parameters. Fig. 10a display the contour plot and the three-dimensional (3D) plot for the interaction effect between A (molar ratio) and B (Catalyst), while the reaction temperature and time were kept constant at 65 °C and 105 min, respectively, throughout the experiments. Fig. 10a shows the contour plot that has higher biodiesel conversion (>60%) was obtained between low and intermediate molar ratio (164.4 to 185.8 M) and between the upper and intermediate catalyst amount (2.5 to 2.2 g). The 3D response surface showed that the conversion of TS to FAME increased with increasing catalyst amount and decreasing molar ratio. At 2.5 g of catalyst and 170.5 molar ratios, a conversion of 60.89% to FAME was achieved. Increasing the molar ratio to 250 reduced the conversion to biodiesel to about 48.50%. This implies that methanol has an inverse relation with biodiesel conversion as described for the reasons stated above.

The contour plot and the three-dimensional (3D) plot for the interaction effect between A (molar ratio) and C (time) are shown in Fig. 10b. The reaction temperature and catalyst amount were kept constant at 65 °C and 1.75 g respectively. Fig. 10b shows the contour plot that has higher biodiesel conversion (> 75%) was obtained at a minimum range molar ratio (143 up to 164.4 molar ratios) and reaction time in the range of 60 min up to 70 min. The 3D response surface shows that the biodiesel product increased with both decreasing reaction time and decreasing molar ratio, which again clearly shows that excess methanol has a significant negative impact on biodiesel conversion as shown by Lee *et al.*[50] The contour plot and the three-dimensional (3D) plot for the interaction effect between B (catalyst) and C (time) are depicted in Fig. 10c. The reaction temperature and molar ratio were kept constant at 65 °C and 196.5 molar ratio respectively. The contour plot Fig. 10c shows that higher biodiesel conversion (>77%) was obtained between an intermediate and high amount of catalyst (2.2 to 2.5) and at low values of time (60 min to 30 min). The 3D response surface supports this. For example, at 60 min and 2.4 g catalyst, the biodiesel conversion was 77.96%, but when the time was increased to 180 min, a major decline in conversion was observed (less than 54%). This indicates that excess reaction time resulted in decreased biodiesel product.

In the present experiment, biodiesel production was set to the maximum value, while the other reaction parameters were set at a minimum value (see Table 10). The experimental conditions with the highest predicted biodiesel value were selected for further validation. The result of model validation is shown in Table 11. An optimum biodiesel conversion of 87.62% was obtained by transesterifying tristearin with 2.5 g of catalyst and a methanol to TS molar ratio of 143 : 1 at 65 °C for 60 min. The experimental product is in good agreement with the predicted value (87.79%) with a relatively small percentage error (0.1936) see Table 11. This shows that the proposed statistical model is suitable for the prediction of optimized biodiesel products and for the optimization of the transesterification process.

In conclusion, the best values of the parameters for the transesterification reaction based on the design of the experiment [DoE] which was performed in the laboratory was 2.5 g of catalyst, molar ratio 143 and 60 min of reaction time [see the result from Table 11]. Table 11 gives the predicted conversion of 87.79% from the DoE simulation in close agreement with the experimental conversion of 87.62%. Thus, compared to our single variable strategy, the DoE resulted in a good optimisation of the transesterification reaction but with milder reaction conditions.

Table 10 Optimization criteria for the transesterification process

Factors	Goal	Lower limit	Upper limit
A: molar ratio	Minimize	143	250
B: catalyst amount	Minimize	1	2.5
C: reaction time	Minimize	60	150
Conversion	Maximize	36.35	87.62

Table 11 Validation model at the optimum conditions

Catalyst (g)	The molar ratio (M)	Time (min)	Experimental Con. (%)	Predicted Con. value (%)	Percentage errors
2.5	143	60	87.62	87.79	0.1936

4. Conclusion

The surface is functionalised basified PANF mesh was shown to be an efficient solid base catalyst in the transesterification process with potential application for biodiesel production. The presence of strongly basic hydrazine groups on the PANF, once protonated, were able to electrostatically bind with Cl^-

and ultimately the Cl^- anion could ion exchange with OH^- ions. The OH^- ions were thus able to react with methanol to produce the methoxide in transesterification. The transesterification reaction parameters of the molar ratio of TS or GMS to alcohol, reaction time, catalyst concentration and temperature were chosen to optimize the synthesis of the methyl ester. This work suggests that methyl esters can be synthesized at high percentage conversion (above 97 w/w%) at 65 °C at a molar ratio of methanol to GMS of 115 : 1, 1 h and 2.5 g basified PANF mesh catalyst in a total volume of 108.95 mL, greater than 95 w/w% conversions was observed at 65 °C with a molar ratio of methanol to tristearin of 285.5 : 1, 2 h and 6 g basified PANF mesh catalyst, total volume 107.48 mL.

RSM was successfully applied to assess the effects of multiple variables, including alcohol/TS molar ratio, catalyst mass and reaction time to produce biodiesel. The Predicted R^2 of 0.9983 is in reasonable agreement with the Adjusted R^2 of 0.9987; *i.e.*, the difference is less than 0.2. In conclusion, the best values of the parameters for the transesterification reaction based on the design of the experiment [DoE] was 2.5 g of catalyst, molar ratio of methanol to TS of 143 : 1 and 60 min of reaction time. The predicted conversion of 87.79% from DoE simulation is in close agreement with the experimental conversion of 87.62%.

Thus, the novel basified PANF catalyst requires a relatively low temperature *i.e.* 65 °C and only a comparatively short reaction time, that is 2 hours to achieve maximum conversion albeit at a higher methanol to TGs molar ratio. However, the methanol is normally recovered in industry and reused back within the transesterification process. This together with the advantages of the surface functionalized PANF solid base catalyst such as its production at industrial quantities, recyclability, ease of use, economic viability, effectiveness, as well as its eco-friendly aspects suggests that it has the potential for transesterification of TGs and hence would be useful in biodiesel production.

Conflicts of interest

There are no conflicts to declare.

Acknowledgements

This work is supported by funding from the co-sponsors Daphne Jackson Trust, Society of Chemical Industry (SCI) and Royal Society of Chemistry (RSC), and hosted at De Montfort University, Leicester. I also thank the technical team (Nazmin and Unmesh) for their help with instrumentation, especially Dr Ketan Ruparelia to run the NMR technique.

References

1 W. Nabgan, A. A. Jalil, B. Nabgan, A. H. Jadhav, M. Ikram and A. Ul-Hamid, *et al.*, Sustainable biodiesel generation through catalytic transesterification of waste sources: a literature review and bibliometric survey, *RSC Adv.*, 2022, **12**(3), 164–1627.

2 D. Samios, F. Pedrotti, A. Nicolau, Q. B. Reiznautt, D. D. Martini and F. M. Dalcin, A Transesterification Double Step Process—TDSP for biodiesel preparation from fatty acids triglycerides, *Fuel Process. Technol.*, 2009, **90**(4), 599–605.

3 C. Urrutia, N. Sangaletti-Gerhard, M. Cea, A. Suazo, A. Aliberti and R. Navia, Two step esterification–transesterification process of wet greasy sewage sludge for biodiesel production, *Bioresour. Technol.*, 2016, **200**, 1044–1049.

4 M. K. Lam, K. T. Lee and A. R. Mohamed, Homogeneous, heterogeneous and enzymatic catalysis for transesterification of high free fatty acid oil (waste cooking oil) to biodiesel: A review, *Biotechnol. Adv.*, 2010, **28**(4), 500–518.

5 K. A. Borges, A. L. Squissato, D. Q. Santos, W. B. Neto, A. C. F. Batista and T. A. Silva, *et al.*, Homogeneous catalysis of soybean oil transesterification via methylic and ethylic routes: Multivariate comparison, *Energy*, 2014, **67**, 569–574.

6 P. Hariprasath, S. T. Selvamani, M. Vigneshwar, K. Palanikumar and D. Jayaperumal, Comparative analysis of cashew and canola oil biodiesel with homogeneous catalyst by transesterification method, *Mater. Today: Proc.*, 2019, **16**, 1357–1362.

7 J. M. Dias, M. C. M. Alvim-Ferraz and M. F. Almeida, Comparison of the performance of different homogeneous alkali catalysts during transesterification of waste and virgin oils and evaluation of biodiesel quality, *Fuel*, 2008, **87**(17), 3572–3578.

8 G. Vicente, M. Martínez and J. Aracil, Optimisation of integrated biodiesel production. Part I. A study of the biodiesel purity and yield, *Bioresour. Technol.*, 2007, **98**(9), 1724–1733.

9 J. K. Efavi, D. Kanbogtah, V. Apalangya, E. Nyankson, E. K. Tiburu and D. Dodoo-Arhin, *et al.*, The effect of NaOH catalyst concentration and extraction time on the yield and properties of Citrullus vulgaris seed oil as a potential biodiesel feed stock, *S. Afr. J. Chem. Eng.*, 2018, **25**(1), 98–102.

10 N. F. Hasanah, Process Parameter Optimisation for Transesterification of Canola Oil using Continuous Reactor with Homogeneous Base Catalyst, *Adv. Sustainable Eng.*, 2021, **01**, 1.

11 A. Munyentwali, H. Li and Q. Yang, Review of advances in bifunctional solid acid/base catalysts for sustainable biodiesel production, *Appl. Catal., A*, 2022, 118525.

12 I. Istadi, S. A. Prasetyo and T. S. Nugroho, Characterization of K2O/CaO-ZnO catalyst for transesterification of soybean oil to biodiesel, *Procedia Environ. Sci.*, 2015, **23**, 394–399.

13 M. Feyzi and L. Norouzi, Preparation, and kinetic study of magnetic Ca/Fe3O4@ SiO2 nanocatalysts for biodiesel production, *Renewable Energy*, 2016, **94**, 579–586.

14 R. Anr, A. A. Saleh, M. S. Islam, S. Hamdan and M. A. Maleque, Biodiesel production from crude Jatropha oil using a highly active heterogeneous nanocatalyst by optimizing transesterification reaction parameters, *Energy Fuels*, 2016, **30**(1), 334–343.

15 M. Prabu, M. Manikandan, P. Kandasamy, P. R. Kalaivani, N. Rajendiran and T. Raja, Synthesis of biodiesel using the Mg/Al/Zn hydrotalcite/SBA-15 nanocomposite catalyst, *ACS Omega*, 2019, **4**(2), 3500–3507.
16 R. Chamola, M. F. Khan, A. Raj, M. Verma and S. Jain, Response surface methodology based optimization of in situ transesterification of dry algae with methanol, H2SO4 and NaOH, *Fuel*, 2019, **239**, 511–520.
17 A. Abubakar, A. A. Mahmoud, D. A. Ajiya, U. F. Hassan, K. Y. Muhammad and S. Aban Sallau, *et al.*, Optimization Process of Parameters for the Transesterification of Jatropha curcas Seed Oil using Response Surface Methodology (RSM), *Int. J. Res. Sci. Innov. Appl. Sci., Volume*, 2022, **VII**(II), 2454.
18 N. H. Zabaruddin, L. C. Abdullah, N. H. Mohamed and T. S. Y. Choong, Optimization using response surface methodology (RSM) for biodiesel synthesis catalyzed by radiation-induced Kenaf catalyst in packed-bed reactor, *Processes*, 2020, **8**(10), 1289.
19 A. Garg and S. Jain, Process parameter optimization of biodiesel production from algal oil by response surface methodology and artificial neural networks, *Fuel*, 2020, **277**, 118254.
20 R. Ahmed and K. Huddersman, Review of biodiesel production by the esterification of wastewater containing fats oils and grease (FOGs), *J. Ind. Eng. Chem.*, 2022, **110**, 1–14, DOI: **10.1016/j.jiec.2022.02.045**.
21 V. V. Ishtchenko, K. D. Huddersman and R. F. Vitkovskaya, Part 1. Production of a modified PAN fibrous catalyst and its optimisation towards the decomposition of hydrogen peroxide, *Appl. Catal., A*, 2003, **242**(1), 123–137.
22 K. I. Doudin, Quantitative and qualitative analysis of biodiesel by NMR spectroscopic methods, *Fuel*, 2021, **284**, 119114.
23 R. A. Ahmed, S. Rashid and K. Huddersman, Esterification of stearic acid using novel protonated and crosslinked amidoximated polyacrylonitrile ion exchange fibres, *J. Ind. Eng. Chem.*, 2023, **119**, 550–573, DOI: **10.1016/j.jiec.2022.12.001**.
24 V. Mandari and S. K. Devarai, Biodiesel production using homogeneous, heterogeneous, and enzyme catalysts via transesterification and esterification reactions: A critical review, *BioEnergy Res.*, 2022, **15**(2), 935–961.
25 J. Otera, Transesterification, *Chem. Rev.*, 1993, **93**(4), 1449–1470.
26 M. V. Rodionova, R. S. Poudyal, I. Tiwari, R. A. Voloshin, S. K. Zharmukhamedov and H. G. Nam, *et al.*, Biofuel production: challenges and opportunities, *Int. J. Hydrogen Energy*, 2017, **42**(12), 8450–8461.
27 E. F. Aransiola, T. V. Ojumu, O. O. Oyekola, T. F. Madzimbamuto and D. Ikhu-Omoregbe, A review of current technology for biodiesel production: State of the art, *Biomass Bioenergy*, 2014, **61**, 276–297.
28 I. M. Rizwanul Fattah, H. C. Ong, T. Mahlia, M. Mofijur, A. S. Silitonga and S. A. Rahman, *et al.*, State of the art of catalysts for biodiesel production, *Front. Energy Res.*, 2020, **8**, 101.
29 L. C. Meher, D. V. Sagar and S. N. Naik, Technical aspects of biodiesel production by transesterification—a review, *Renewable Sustainable Energy Rev.*, 2006, **10**(3), 248–268.
30 N. Rasimoglu and H. Temur, Cold flow properties of biodiesel obtained from corn oil, *Energy*, 2014, **68**, 57–60.
31 F. Ezebor, M. Khairuddean, A. Z. Abdullah and P. L. Boey, Oil palm trunk and sugarcane bagasse derived heterogeneous acid catalysts for production of fatty acid methyl esters, *Energy*, 2014, **70**, 493–503.
32 M. Satyanarayana and C. Muraleedharan, A comparative study of vegetable oil methyl esters (biodiesels), *Energy*, 2011, **36**(4), 2129–2137.
33 J. M. Encinar, A. Pardal and G. Martínez, Transesterification of rapeseed oil in subcritical methanol conditions, *Fuel Process. Technol.*, 2012, **94**(1), 40–46.
34 M. A. Olutoye, S. W. Wong, L. H. Chin, H. Amani, M. Asif and B. H. Hameed, Synthesis of fatty acid methyl esters via the transesterification of waste cooking oil by methanol with a barium-modified montmorillonite K10 catalyst, *Renewable Energy*, 2016, **86**, 392–398.
35 J. M. Encinar, J. F. González, A. Pardal and G. Martínez, Rape oil transesterification over heterogeneous catalysts, *Fuel Process. Technol.*, 2010, **91**(11), 1530–1536.
36 A. A. Koutsouki, E. Tegou, A. Badeka, S. Kontakos, P. J. Pomonis and M. G. Kontominas, In situ and conventional transesterification of rapeseeds for biodiesel production: The effect of direct sonication, *Ind. Crops Prod.*, 2016, **84**, 399–407.
37 N. Chumuang and V. Punsuvon, Response surface methodology for biodiesel production using calcium methoxide catalyst assisted with tetrahydrofuran as cosolvent, *J. Chem.*, 2017, **2017**, 1–9, DOI: **10.1155/2017/4190818**.
38 Y. H. Tan, M. O. Abdullah, C. Nolasco-Hipolito and Y. H. Taufiq-Yap, Waste ostrich-and chicken-eggshells as heterogeneous base catalyst for biodiesel production from used cooking oil: Catalyst characterization and biodiesel yield performance, *Appl. Energy*, 2015, **160**, 58–70.
39 A. S. Yusuff, O. D. Adeniyi, S. O. Azeez, M. A. Olutoye, U. G. Akpan, A. S. Yusuff, O. D. Adeniyi, S. O. Azeez, M. A. Olutoye and U. G. Akpan, Synthesis and characterization of anthill-eggshell-Ni-Co mixed oxides composite catalyst for biodiesel production from waste frying oil, Biofuels, Bioproducts and Biorefining, UK, 13: 37-47, 2019, Online ISSN: 1932-1031, DOI: **10.1002/bbb.1914**.
40 N. Boz, N. Degirmenbasi and D. M. Kalyon, Esterification and transesterification of waste cooking oil over Amberlyst 15 and modified Amberlyst 15 catalysts, *Appl. Catal., B*, 2015, **165**, 723–730.
41 T. Dong, J. Wang, C. Miao, Y. Zheng and S. Chen, Two-step in situ biodiesel production from microalgae with high free fatty acid content, *Bioresour. Technol.*, 2013, **136**, 8–15.
42 J. M. Encinar, J. F. González, G. Martínez and S. Nogales-Delgado, Use of NaNO3/SiAl as Heterogeneous Catalyst for Fatty Acid Methyl Ester Production from Rapeseed Oil, *Catalysts*, 2021, **11**(11), 1405.

43 L. Hsieh, U. Kumar and J. C. Wu, Continuous production of biodiesel in a packed-bed reactor using shell–core structural Ca (C3H7O3) 2/CaCO3 catalyst, *Chem. Eng. J.*, 2010, **158**(2), 250–256.
44 C. A. Akinremi, S. Rashid, P. D. Upreti, G. T. Chi and K. Huddersman, Regeneration of a deactivated surface functionalised polyacrylonitrile supported Fenton catalyst for use in wastewater treatment, *RSC Adv.*, 2020, **10**(22), 12941–12952.
45 Y. C. Wong, Y. P. Tan, Y. H. Taufiq-Yap and I. Ramli, An optimization study for transesterification of palm oil using response surface methodology (RSM), *Sains Malays.*, 2015, **44**(2), 281–290.
46 S. H. Shuit, K. T. Lee, A. H. Kamaruddin and S. Yusup, Reactive extraction of Jatropha curcas L. seed for production of biodiesel: process optimization study, *Environ. Sci. Technol.*, 2010, **44**(11), 4361–4367.
47 N. G. Zanjani, A. Kamran-Pirzaman and M. Khalajzadeh, Synthesis of modified layered double hydroxide of MgAl catalyst with Ba and Li for the biodiesel production, *Clean Technol. Environ. Policy*, 2020, **22**, 1173–1185.
48 P. Goyal, M. P. Sharma and S. Jain, Optimization of transesterification of Jatropha curcas oil to biodiesel using response surface methodology and its adulteration with kerosene, *J. Mater. Environ. Sci.*, 2013, **4**(2), 277–284.
49 M. K. Yesilyurt, M. Arslan and T. Eryilmaz, Application of response surface methodology for the optimization of biodiesel production from yellow mustard (Sinapis alba L.) seed oil, *Int. J. Green Energy*, 2019, **16**(1), 60–71.
50 H. V. Lee, R. Yunus, J. C. Juan and Y. H. Taufiq-Yap, Process optimization design for jatropha-based biodiesel production using response surface methodology, *Fuel Process. Technol.*, 2011, **92**(12), 2420–2428.